# Sympathetic nervous system and locomotor integration from V3 spinal neurons

by

Camila Chacon

A thesis submitted to the Faculty of Graduate Studies of
The University of Manitoba
in partial fulfillment of the requirements of the degree of

MASTER OF SCIENCE

Faculty of Physiology and Pathophysiology
University of Manitoba
Winnipeg

## Abstract

Approximately 80,000 individuals live with spinal cord injury (SCI) in Canada. Dysregulation of sympathetic function is common after SCI because communication between autonomic centres and spinal sympathetic outflow is lost due to the intervening injury. However, sympathetic preganglionic neurons (SPNs) located in the intermediate lamina (IML) of T1-L2 spinal cord (SC) retain spontaneous activity, and lumbar electrical stimulation appears to increase thoracic sympathetic output and cardiovascular function after cervical SCI. The source of this excitatory neuronal input to SPNs is unknown. We hypothesized that ascending propriospinal interneurons (INs) located in the lumbar SC synapse with and provide excitatory drive to thoracic SPNs (tSPNs). We tested our hypothesis examining innervation patterns from lumbar V3 INs on tSPNs in Sim1CreTdTomato mice. To characterize the distribution of V3 INs, we counted and determined soma location in transverse sections of thoracic and lumbar SC. To determine if lumbar V3 INs show distinct innervation patterns to tSPNs, BDA was injected near the central canal into L1-L5 segments. To investigate which V3 IN populations were responsible for input to T8 (mediating sympathetic output to adrenal glands), CTB was injected targeting the IML. One-week post-surgery, mice were euthanized, SCs were harvested and processed for immunohistochemistry. IMARIS Bitplane was used to generate and quantify 3-dimensional reconstructions of tSPNs and synaptic contacts. Of all excitatory VGlut2 input apposing tSPNs, ~20% arose from V3 IN projections ($TdTom^+/VGlut2^+$, n = 4 mice). L2 BDA injections resulted in 2x more contacts in T1-6 versus T7-T12, whereas L4/5 BDA injections resulted in 2.6x more contacts in T7-T12 ($BDA^+/TdTom^+$). Injections of CTB targeting T8 IML revealed that ipsilateral (74%, 55%, 63%) and contralateral (67%, 55%, 67%; $V3_D$, $V3_{intermediate}$, $V3_V$ respectively) V3 INs in L1-6 provided input to T8 (n = 4 mice). This is the first demonstration that spinal neurons involved in locomotion provide direct synaptic input to SPNs and may suggest locomotor function is intrinsically integrated with sympathetic autonomic functions at the level of the SC. In future, these findings may help direct spinal electrical stimulation studies aimed at improving not only locomotor function, but autonomic function and life quality in SCI individuals.

## Acknowledgements

I would like to thank my supervisor **Dr. Jeremy Chopek** for accepting me as your student while COVID-19 unfolded around us. I still think you took a chance on me, but I am truly glad you did! Thank you for your calm, collected nature and guidance. I truly appreciate everything you have done and taught me. This project would not have come to fruition without all your help and patience. I would also like to thank my committee members, **Drs. Kristine Cowley** & **Katinka Stecina**. Katinka, my mind was constantly fed with new ideas and my stomach with cake! Kris, I don't know how whenever I would ask a brief question, it would turn into a long conversation with many asides and maybe the original question would be answered somewhere in there too. Thank you to everyone at the SCRC, particularly **Antonia**, for the immuno troubleshooting at the beginning of my project, **Katrina** for your shared interest in true crime and golfing. Thank you, **Shannon**, for all your technical advice. Thank to my fellow lab members **Narjes**, **Victoria, Lucia** and **Muniza**. Thank you to everyone at **KIAM** and the **Nagy** lab for microscope access and help with imaging.

Thank you to my family, **Hernando**, **Olga** & **Stella**. Gracias por todo el apoyo que me han dado toda mi vida en todo lo que hago, los quiero mucho mucho. It must be stressful to constantly have your only child in different provinces, but I am so grateful for being given the liberty to do so.

Thank you to my Winnipeg family, I cannot express how grateful I am to have been adopted in as the little kid. Thank you, **Karla**, la verdad no sé qué haría hecho sin ti — jamás pensé conocer alguien que consideraría mi hermana mayor y siempre lo serás. ¡Mil gracias por todo el apoyo! Thank you, **Santiago**, for being forced into a friendship with me and being such a good sport about everything. Thank you, **Ana**, for teaching me how to salsa, thank you **Mara** for having invited me to that first First Friday, thank you, **Ally** for being my #1 hype person, thank you, **Heather** for your laugh and big pharma help, and thank you **Mariel** for being the best neighbour!

Thank you to my **RDCSC** squad, **Kris**, **Dina** and **Amber**, for teaching me teamwork, grit, and perseverance.

Thank you to my **McGill** family, COVID cut our time short, but I am thankful for all the beautiful memories, nonetheless. There are *way too many* of you to list, but you know who you are.

Thank you to **all** my Red Deer friends for always being interested in my scientific endeavours. Special shoutout to **Jill** for always being down to listen to me practice my Zoom presentations even if you fell asleep during them.

Thank you to **everyone** I may have missed, your support didn't go unnoticed, I just have a page of thank yous, and as you all know, I am a very social butterfly ☺. As an only child I have been lucky to choose my family and for that I have been extremely grateful. It takes a village.

"Try again. Fail again. Fail better" – Samuel Beckett

## Dedication

To all the frontline workers and scientific community, your sacrifices during the COVID-19 pandemic made it possible for me to continue my studies, culminating in this thesis.

To my parents, who always encourage me to explore my scientific interests.

To François & Olivia, for being the best study buddies.

In loving memory of Gabriela, Petunia, Emilia & Luca.

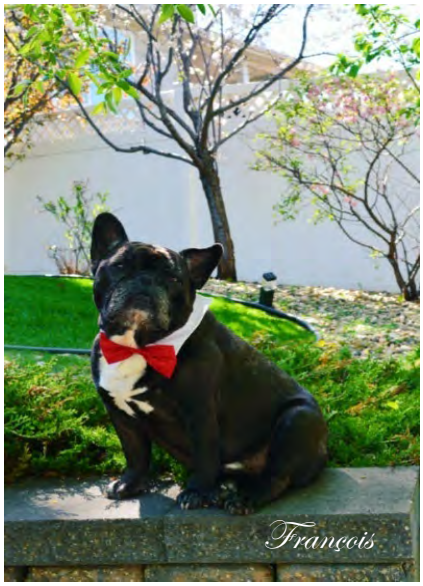






# Table of Contents

*Abstract* ..... *ii*

*Acknowledgements* ..... *iii*

*Dedication* ..... *iv*

*List of Tables* ..... *vii*

*List of Figures* ..... *viii*

*List of Acronyms/Abbreviations* ..... *ix*

*Chapter I: Introduction* ..... *1*

*Chapter II: Overview of spinal cord injury and its effects on locomotion and sympathetic function* ..... *5*

**2.1 Spinal Cord Injury** ..... **5**

**2.2 Autonomic Nervous System** ..... **6**

**2.2.1 Sympathetic Preganglionic Neurons** ..... 8

**2.2.2 Autonomic Dysreflexia (AD)** ..... 13

**2.3 Mesencephalic Locomotor Region (MLR)** ..... **16**

**2.4 Central Pattern Generators** ..... **16**

**2.5 Propriospinal Interneurons (INs)** ..... **18**

**2.5.1 V3 Propriospinal Interneurons** ..... 22

**2.6 Epidural Stimulation (ES)** ..... **24**

**2.7 Mouse Genetics** ..... **25**

**2.8 Project Rationale** ..... **26**

**2.9 Hypotheses & Aims** ..... **28**

**2.9.1 Overarching Hypothesis:** ..... 28

**2.9.2 Specific Aims & Aim Hypotheses** ..... 28

*Chapter III: Methods* ..... *29*

**3.1 Ethics Declaration** ..... **29**

**3.2 Animals & Mouse Genetics** ..... **29**

**3.3 Experimental Design** ..... **29**

**3.3.1 Defining anterograde and retrograde tracers** ..... 29

**3.3.2 Biotin-dextran Amine (BDA) Tracer** ..... 30

**3.3.3 Cholera Toxin Subunit B (CTB) Tracer** ..... 30

**3.3.4 Surgical Procedures** ..... 31

**3.3.5 Stereotaxic Injections** ..... 31

**3.3.6 Spinal Cord Harvesting & Sectioning** ..... 33

**3.3.7 Immunohistochemistry** ..... 33

**3.3.8 Microscopy & Image Analysis** ..... 37

**3.3.9 Statistical Analysis** ..... 39

*Chapter IV: Results* ..... *41*

**4.1 Distribution of V3 INs within the thoraco-lumbar spinal cord .....41**
**4.2 Projections of V3 INs.....51**
***Chapter V: Discussion..... 63***
**5.1 Summary of results .....63**
**5.2 V3 soma and puncta distribution in the thoraco-lumbar spinal cord.....63**
**5.3 Functionality of VGlut2 input on SPNs .....67**
**5.4 Projections of different populations of V3 INs.....69**
**5.5 Investigating other IN subtypes that may appose thoracic SPNs .....72**
**5.6 Limitations.....73**
***Chapter VI: Conclusion ..... 75***
**6.1 Key Findings .....75**
**6.2 Future Directions .....76**
***References ..... 78***
***Appendix..... 86***
**Tris-EDTA buffer recipe for antigen retrieval:.....86**
**Table 1: List of items and reagents .....87**
**Table 2: List of Antibodies and RRIDs .....89**
**Post-Surgery Score Sheet Parameters.....90**
**Table 3: Post-surgical monitoring schedule based on scores. .....91**

# List of Tables

TABLE 1 ..... 21
TABLE 2 ..... 36
TABLE 3 ..... 71

# List of Figures

FIGURE 1 ..... 11
FIGURE 2 ..... 12
FIGURE 3 ..... 15
FIGURE 4 ..... 40
FIGURE 5 ..... 42
FIGURE 6 ..... 44
FIGURE 7 ..... 47
FIGURE 8 ..... 49
FIGURE 9 ..... 53
FIGURE 10 ..... 54
FIGURE 11 ..... 58
FIGURE 12 ..... 59
FIGURE 13 ..... 60
FIGURE 14 ..... 62

## List of Acronyms/Abbreviations

**AD** (autonomic dysreflexia)

**AHP** (afterhyperpolarization)

**ANS** (autonomic nervous system)

**AP** (action potential)

**BDA** (biotin-dextran-amine)

**BP** (blood pressure)

**CAN** (central autonomic nuclei)

**ChAT** (choline acetyltransferase)

**CNS** (central nervous system)

**CPG** (central pattern generator)

**CTB** (cholera toxin subunit B)

**CTB-A488** (cholera toxin subunit B Alexa 488)

**DLR** (diencephalic locomotor region)

**E** (epinephrine)

**ES** (Epidural stimulation)

**IHC** (immunohistochemistry)

**IML** (intermediate lamina)

**IN** (interneuron)

**KO** (knockout)

**medRF** (medial reticular formation)

**MIP** (maximum intensity projection)

**MLR** (mesencephalic locomotor region)

**NE** (norepinephrine)

**NO** (nitric oxide)

**PBS** (phosphate buffered saline)

**PBS-T** (phosphate buffered saline – triton)

**PFA** (paraformaldehyde)

**RS** (reticulospinal)

**RSN** (reticulospinal neuron)

**RT** (room temperature)

**SC** (spinal cord)

**SCI** (spinal cord injury)

**Sim1** (simpled-minded1)

**SNS** (sympathetic nervous system)

**SPN** (sympathetic preganglionic neuron)

**tSPN** (thoracic sympathetic preganglionic neuron)

**TeNT** (tetanus light chain)

**TF** (transcription factor)

**VGlut2** (vesicular glutamate transporter 2)

**VLF** (ventrolateral funiculus)

## Chapter I: Introduction

In an able-bodied world, it is easy to take locomotion for granted. When we walk or run, we are instructing our spinal cord to activate muscle groups in a precise manner to elicit a behavioural output (Chopek, Zhang & Brownstone, 2021). Sensory and motor processes within the spinal cord are influenced by descending systems of the brain (Du Beau et al., 2012), mostly through coordination of various brain systems such as basal ganglia, midbrain, cerebellum and brainstem motor centres (Svoboda, 2018) converging on the spinal cord and motoneurons to elicit movement. However, rhythmic locomotion is not only controlled by higher functioning areas, such as the motor cortex (Kawai et al, 2015), but foundationally, through robust pattern generators located within the spinal cord.

Organizational principles of locomotion are conserved among multiple species such that neuronal circuits and neural mechanisms produce and coordinate multiple locomotor patterns (Grillner & Kozlov, 2021). These organizational principles involved in execution of an appropriate motor response, underly survival and are one of the fundamental aspects of the nervous system (Jung & Dasen, 2015). Locomotion is a semi-automated task (Sylos-Labini et al., 2017) designed for exploratory and escape behaviours, driven by central pattern generators (CPGs). Excitation of the mesencephalic locomotor region (MLR) has been shown to initiate locomotion through descending drive that projects to reticulospinal (RS) neurons which in turn project to neurons comprising locomotor CPGs in cervical and lumbar enlargements of the spinal cord (Shik, Severin & Orlovsky, 1966). These experiments have allowed the development of understanding underlying neural pathways and mechanisms contributing to the production and coordination of movement.

Electrophysiological and lesioning studies suggest that circuitry producing and coordinating locomotion are distributed throughout the spinal cord. Using field potential and intracellular recordings, Alstermark and colleagues (1979) showed that cervical propriospinal neurons located in the spinal cord coordinate forelimb-hindlimb function (Alstermark et al., 1979). Multiple lesioning experiments also demonstrated a distributed network in which spinal neurons can generate rhythmic locomotion (Cowley & Schmidt, 1997; Cazalets, Borde & Clarac, 1995). Ultimately, these locomotor outputs and activities relay ascending and descending command signals in the spinal cord which contribute to activation of the sympathetic network (Juvin, Simmers & Morin, 2005; Zaporozhets, Cowley & Schmidt, 2006; Cowley, Zaporozhets & Schmidt, 2008, 2010).

The sympathetic nervous system (SNS) regulates firing rates in tonically active SPNs, which in turn, provide excitatory input to the body tissues and organs including the heart, peripheral vasculature and adrenal glands in response to changes in the external or internal environment (Kandel, 2013). Normally, descending signals originating from hypothalamus and medulla increase excitatory input to neurons in the SNS during movement and exercise to increase activity levels in multiple tissues and organs, including the adrenal glands (Kandel, 2013; Kingsley & Figueroa, 2014) through sympathetic preganglionic neurons (SPNs). SPNs are the source of sympathetic outflow to the periphery and are located in the intermediate lamina (IML) of thoracic and upper lumbar spinal segments (T1-L2) (Loewy & Spyer, 1990; Llewellyn-Smith, 2009).

Spinal cord injury (SCI) affects the ability to maintain robust and patterned locomotor activity depending on its severity and location. The severity of injury is determined by the number of supraspinal descending fibres, ascending fibres and neurons in grey matter at site of injury that remain intact, and the level of injury within in the spinal cord (Hou & Rabchevsky, 2014). For example, a spinal cord injury at T12 would result in lower limb paralysis but an intact sympathetic system with the ability to activate thoracic SPNs, whereas an injury above T1 would result in paralysis of all limbs and the inability to activate thoracic SPNs. The resultant paralysis and potential lack of sympathetic output leaves a person living with SCI at a significant risk of a multitude of secondary complications, such as cardiovascular and autonomic dysfunction, which will be discussed later.

Considering that descending drives are present for both locomotor and sympathetic function and that sympathetic output increases in response to locomotion, it is likely that there is cellular connectivity mediating the two systems. Integration between locomotor and sympathetic centres is observed in the brainstem, but this communication is lost after injury. However, there have been instances in which ascending control from lumbar spinal segments can coordinate and integrate movement without brainstem spinal centres (Juvin, Simmers & Morin, 2005). Few studies have examined the targets of propriospinal neuron projections (Brockett et al., 2013), let alone the characterization of integration between spinal neurons or circuits responsible for locomotor and sympathetic integration (Cowley, 2018) in the ascending direction. We believe this involves propriospinal neurons and that integration likely occurs between locomotor neurons and SPNs, like that seen in the brainstem. Therefore, we hypothesize that locomotor-related and

rhythmically active propriospinal interneurons have long ascending projections to sympathetic nuclei throughout the thoracic spinal cord.

Through advancements in mice genetics, categorization of cardinal classes of spinal interneurons have been investigated based on transcription factor profiles they express. The use of these mouse models allows for visualization and manipulation of distinct classes of spinal INs to understand their role in locomotion (Goulding, 2009). V3 INs are one of the ten cardinal classes of INs and have been shown to be responsible for robust rhythmic activity observed coordinating left-right sides in locomotion (Zhang et al., 2008), while also having long ascending projections (Blacklaws et al., 2015). Using the Sim1CreTdTomato mouse, we will investigate if V3 INs provide direct synaptic input to neurons within sympathetic nuclei in the thoracic cord. This exploratory project encompasses foundational physiology to investigate if there is anatomical evidence that V3 INs may be involved in coordinating sympathetic and locomotor systems. Thus, these long projections from V3 INs may innervate thoracic SPNs to modulate sympathetic activity during rhythmic activity in locomotion.

# Chapter II: Overview of spinal cord injury and its effects on locomotion and sympathetic function

## 2.1 Spinal Cord Injury

Spinal cord injury (SCI) affects ~ 85,500 individuals in Canada (Noonan et al., 2012) with 42.6 per million (2003-2007) Manitobans added each year (McCammon & Ethans, 2011). SCI etiology includes fall related injuries in individuals 65 years or older (Jain et al., 2015), vehicular accidents (Devivo, 2012), and firearm injuries (Jain et al., 2015). Since etiology of injury is diverse, the variability of SCI can also differ in terms of severity, the location at which the injury occurs, the extent of remaining or spared tissue and type of spinal injury sustained (i.e., crush, contusion etc, Cowley, 2018; Hou & Rabchevsky, 2014; McCammon & Ethans, 2011; McKay et al., 2011a). Although an injury to the spinal cord may be considered "neurologically complete", meaning that there is loss of motor and sensory function below the level of injury, most SCIs are anatomically incomplete, as there is sparing of some white matter. This sparing may provide a bridge to bypass the site of injury and may provide a means to activate circuitry remaining intact below the level of injury (Shepard et al., 2021).

Following a SCI, interneurons that modulate motoneuron excitability suffer loss of synaptic connections in the "immediate injury zone" and connections with supraspinal neural structures are lost/severed (McKay et al., 2011a). Not only do individuals with SCI live with lost sensory-motor function (McKay et al., 2011b), they also are likely to have autonomic dysfunction (Hou & Rabchevsky, 2014) and secondary complications such as cardiovascular dysregulation (Eckert & Martin, 2017) based on the level of injury. For example, those injured above T1 would not be able to increase SNS drive to the heart whereas those with injury below

T6 would. Currently, cardiovascular dysfunction is the leading cause of mortality and morbidity in people living with SCI (Hou & Rabchevsky, 2014). Ultimately, the goal for individuals living with SCI is to restore movement after injury to reduce the burden of disease and secondary complications that arise from insufficient exercise and movement.

Regaining function after injury can help foster greater independence, resulting in an improved quality of life for SCI individuals, and may also improve autonomic function (Harkema et al, 2011). In turn, this may reduce autonomically associated complications. Currently, the majority of SCI research is directed at improving locomotor function (Gómara-Toldrà, Sliwinski & Dijkers, 2014), however, people living with SCI rank improving lost autonomic functions a higher priority than regaining locomotor function (Anderson, 2004; French, Anderson-Erisman & Sutter, 2010;  Simpson et al., 2012; van Middendorp et al., 2016). This emphasizes the need for research to understand how anatomical connections of sympathetic circuitries may be activated to improve autonomic function following SCI.

## 2.2 Autonomic Nervous System

The autonomic nervous system (ANS) is comprised of the sympathetic, parasympathetic, and enteric systems, where the sympathetic and parasympathetic systems maintain homeostasis (Cowley, 2018; Loewy & Spyer, 1990; Widmaier, Raff & Strang, 2014). The SNS is referred to the “fight or flight” system whereas the parasympathetic system is referred to as the “rest and digest” system. The ANS adjusts blood flow, cardiac output and can modulate the respiratory system to meet changes in metabolic and thermoregulatory demands (Wehrwein, Orer & Barman, 2016; Kandel, 2013). When there is increased need of metabolic support, the

hypothalamus relays a signal to autonomic centres in the brainstem to activate the SNS, which increases blood pressure, cardiac output and inhibits the parasympathetic system. When a perceived threat is no longer present, following the activation of the fight or flight response, signals are sent to the brainstem to suppress the SNS and activate the parasympathetic system (Kandel, 2013).

It is important to note the distinct differences between the sympathetic and parasympathetic systems and how SCI impacts function differently within each system. Parasympathetic preganglionic neurons are found in brainstem and sacral regions of the spinal cord, exit the brainstem through cranial nerves III, VII, IX and X, and project to postganglionic neurons in the ciliary, pterygopalatine, submandibular and otic ganglia. Preganglionic fibres from cranial nerve X project to postganglionic neurons in the abdomen such as the stomach, liver and intestinal tract. In the sacral spinal cord, parasympathetic neurons exit through the ventral roots and project to the pelvic ganglion plexus that innervate the colon, bladder and genitalia (Kandel, 2013). In contrast, sympathetic preganglionic neurons cluster in a chain of sympathetic ganglia throughout T1-L2 spinal segments (**Figure 1, 2**; Kandel, 2013). The axons of these neurons exit the spinal cord in the ventral root and extend in the spinal nerve where they separate from somatic motor axons. Axons of preganglionic neurons exit the spinal cord at the level at which their somas are located but may innervate sympathetic ganglia either more rostrally or caudally by travelling in the sympathetic trunk that connects the ganglia. Postganglionic cells that innervate the head are found in the superior cervical ganglion and the rest travel in spinal nerves to their targets (Kandel, 2013). Normally, these two systems work together in balance to maintain homeostasis, however, following SCI, neurons of the parasympathetic system remain

functional (until vagus nerve input) as their somas are not located in the spinal cord, but rather, in the brainstem and post-ganglionic nuclei located outside the vertebral column. In contrast, the sympathetic system is greatly disrupted due to the interruption of signals from descending fibres of supraspinal autonomic centres (Hou & Rabchevsky, 2014; Cowley, 2018; Kandel, 2013; Wehrwein, Orer & Barman, 2016). If the parasympathetic and sympathetic systems can no longer interact with each other, this can cause a variety of issues for SCI individuals, particularly when it comes to maintaining homeostasis or autonomic balance.

### 2.2.1 Sympathetic Preganglionic Neurons

Sympathetic preganglionic neurons (SPNs) are the source of sympathetic input to the periphery, providing drive to postganglionic neurons in sympathetic ganglia (Llewellyn-Smith, 2009; Schober & Unsicker, 2001). SPNs are located in the intermediate lamina (IML) (Llewellyn-Smith, Weaver & Keast, 2006; Llewellyn-Smith, 2009) of the thoracic and upper lumbar spinal cord (T1-L2) (Cowley, 2018; Hou & Rabchevsky, 2014; Llewellyn-Smith, 2009; Loewy & Spyer, 1990). SPNs are cholinergic, use the neurotransmitter acetylcholine (ACh) and can be identified based on immunohistochemical staining for choline acetyltransferase (ChAT), an enzyme that synthesizes ACh (Schober & Unsicker, 2001). Finally, SPNs are defined as neurons whose somas project directly onto post-ganglionic neurons located outside the spinal cord.

Synaptic vesicles immunoreactive for glutamate, GABA and glycine synapse on SPNs (Llewellyn-Smith, Weaver & Keast, 2006). Although normally, a significant portion of input to SPNs arises from supraspinal inputs, SCI transections do not result in deprivation of glutamate to SPNs (Llewellyn-Smith, Weaver, & Keast, 2006). Intraspinal neurons provide glutamatergic

input to SPNs, and following SCI, SPNs can be regulated or influenced by interneurons residing within the spinal cord through complex integration involving mono- and polysynaptic pathways when supraspinal input is absent (Eldahan & Rabchevsky, 2018). This information suggests that intraspinal neurons have glutamatergic anatomical connections on thoracic SPNs.

Three types of SPNs are involved in innervating the cervical ganglia, stellate ganglion, and adrenal medulla. These ganglia are important in regulating sympathetic function of the bronchi and lungs, heart and regulating catecholamine release, respectively (Kandel, 2013). The predominant type of SPNs in the IML are a combination of round and fusiform soma SPNs intermingled within the region and a larger SPN type being less common. **Figure 1** immunohistochemical staining shows round and fusiform SPN somas located in the thoracic IML (**Figure 1**; Schober & Unsicker, 2001; Llewellyn-Smith, 2009). The segmental organization of SPNs and extensive longitudinal dendrites form “ladder-like” motifs (Loewy & Spyer, 1990, Widmaier, Raff & Strang, 2014; Schober & Unsicker, 2001; **Figure 2**) when observed in horizontal/coronal sections (Schober & Unsicker, 2001; Llewellyn-Smith, Weaver, & Keast, 2006). T1-T5 SPNs innervate the heart and are responsible for increasing heart rate, stroke volume and contractility during movement and exercise (Cowley, 2018). T6-T9 SPNs innervate the adrenal glands and are responsible for the release of catecholamines, epinephrine and norepinephrine (E and NE respectively) (**Figure 3**).

It has been shown that immediately following a complete transection at T4/T5, SPN soma size and dendritic lengths in the mid thoracic region are reduced due to degeneration and clearance from the IML of axons detached from their somas. However, 14 days post-transection,

these changes are absent (Llewellyn-Smith, Weaver & Keast, 2006). It is unlikely that reinnervation sprouts regrowth of dendrites following injury to SPNs but growth-associated protein 43, a marker for regenerating axons, remains present in the spinal cord after injury for as long as 6 weeks. Normally, somatic motor and sympathetic systems are tightly integrated at the level of spinal afferents (Sato, 1997). However, morphological changes in SPNs following SCI and absence of supraspinal inhibitory effects may result in changes to SPN activity and may underly episodes of autonomic dysreflexia (Llewellyn-Smith, Weaver & Keast, 2006). This unchecked activity of reflexes regulated by SPNs when supraspinal inhibitory effects on spinal circuits are lost can lead to autonomic dysreflexia (Weaver et al., 2002).

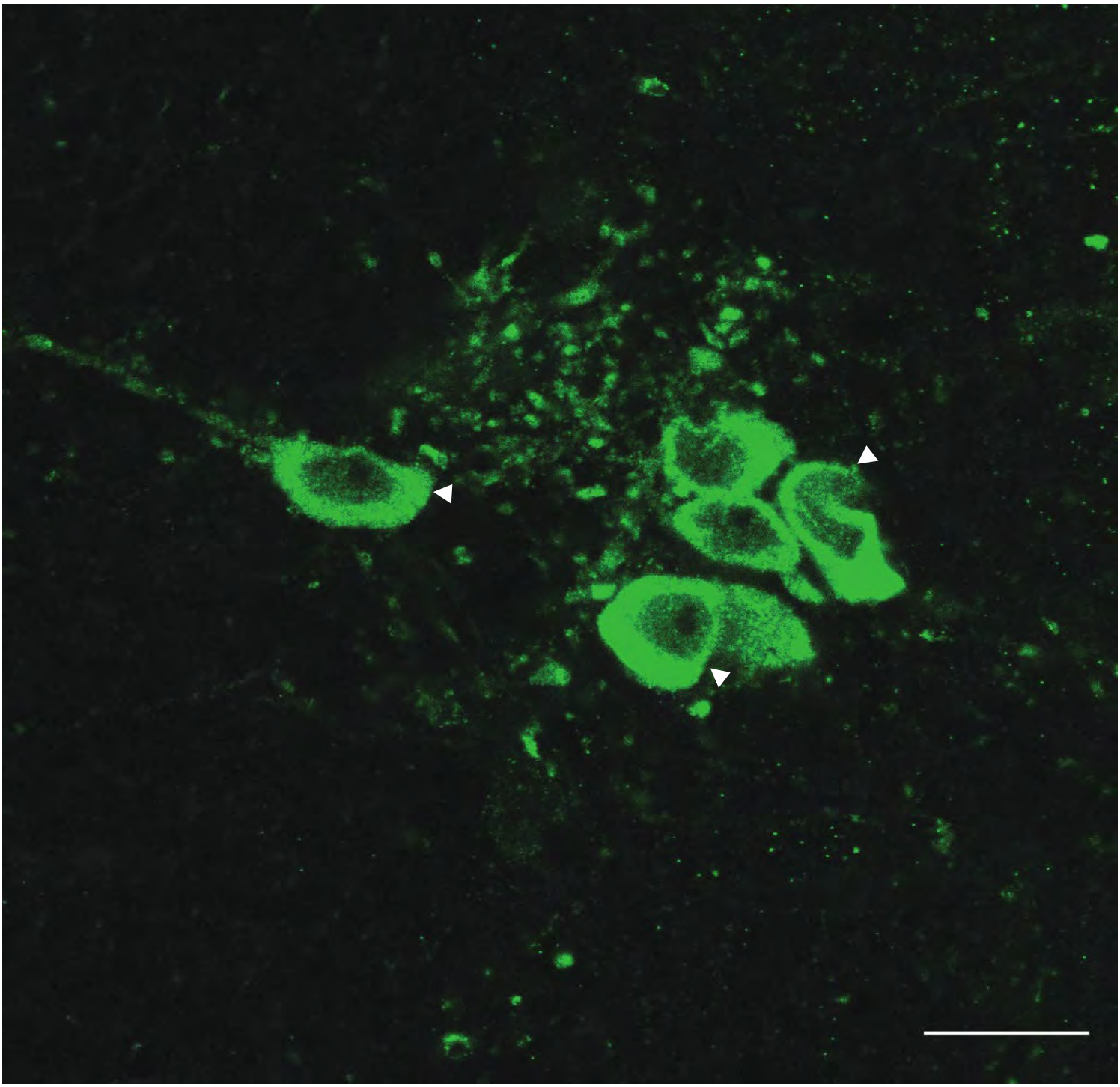

**Figure 1**: **Round and fusiform SPNs located in the thoracic IML.** SPNs are stained with ChAT-A488 (green) in the Sim1CreTdTomato mouse. Round (middle, lower arrowhead) and fusiform (left-most and right-most arrowheads) soma are intermingled in the region. **Scale** = 10 µm.

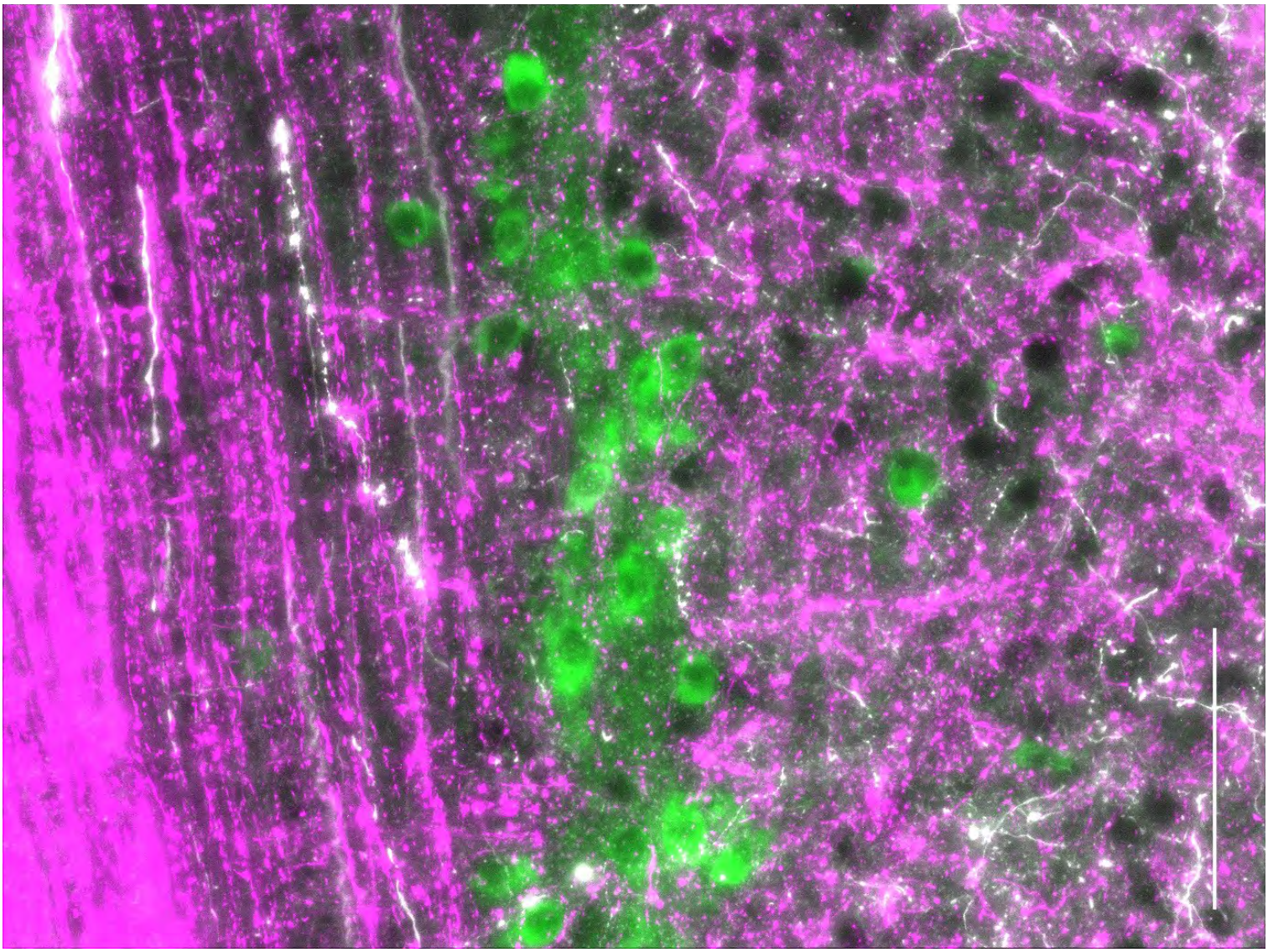

**Figure 2: Ladder-like clusters of SPNs and V3 IN puncta in IML mouse spinal cord.** V3 IN contacts (Cy3, violet) observed in the thoracic IML apposing ladder-like SPN clusters (A488, green) in horizontal 18 µm section with BDA anterograde tracer (Streptavidin 647, white). **Scale** = 100 µm.

### 2.2.2 Autonomic Dysreflexia (AD)

The first period after SCI is known as the “spinal shock” where loss of descending control causes significantly reduced blood pressure (BP) and reduction of sympathetic reflexes, but over time, spinal circuitry reorganization contributes to hyper-excitability and aberrant activation of SPNs and motoneurons (Eldahan & Rabchevsky, 2018). The leading cause of mortality and morbidity in individuals with SCI are cardiovascular associated complications and diseases that arise post-injury (Hou & Rabchevsky, 2014; Savic et al., 2017; Chopra et al., 2018). A common cardiac complication associated with SCI is autonomic dysreflexia (AD) if injury occurs above T6 (Eldahan & Rabchevsky, 2018). The prevalence of AD after SCI when an individual has an injury at or above T6 ranges between 48-91% and this variability may be due to differences in SCI completeness, time that has passed since injury and differences in diagnostic criteria which are used to confirm AD (Eldahan & Rabchevsky, 2018). In people living with SCI, AD does not typically appear until 3-6 months post injury.

In an intact system, supraspinal neurons modulate tonic firing of SPNs and these SPNs innervate peripheral ganglia or the adrenal medulla directly. Sympathetic ganglia innervate blood vessels throughout the body whereas stimulation of the adrenal medulla oversees the release of epinephrine (E) and norepinephrine (NE). Overall, this provides control of blood vessel diameter and peripheral resistance to maintain BP regulation. AD occurs in response to a noxious visceral or somatic stimulation below the level of injury. This results in an increase in sympathetic activity as a reflex, where increased sympathetic outflow causes vasoconstriction in lower parts of the body, resulting in increased arterial BP. Elevated BP is sensed in the carotid bodies, integrated at the level of the rostroventral medulla, resulting in vagal stimulation to increase

parasympathetic outflow. This increased parasympathetic outflow is paired with a reduction of the SNS in the sympathetic chain of the spinal cord to regulate and reduce BP. However, in SCI individuals, input from supraspinal centres is reduced or absent. Thus, SPNs located below the level of injury do not receive descending inhibitory signals from supraspinal BP integration centres and therefore continue to stimulate and constrict blood vessel smooth muscle, resulting in sustained increases in BP. It is only when the noxious stimulus is removed that elevated BP is alleviated. Severe cases of AD can result in coma, epileptic seizures and death (Eldahan & Rabchevsky, 2018; Rabchevsky, 2006; Hou & Rabchevsky, 2014).

Clinically, there are a variety of interventions used to treat an acute hypertensive crisis during a bout of AD, most of which aim to relax smooth muscle. Nitrates are commonly prescribed because they are converted to or release nitric oxide (NO), relaxing smooth muscle vasculature and reducing BP (Eldahan & Rabchevsky, 2018). Nifedipine is an L-type calcium ($Ca^{2+}$) channel blocker also commonly prescribed as it reduces influx of $Ca^{2+}$ into vascular smooth muscle thereby reducing peripheral resistance and therefore BP. There are other interventions as reviewed by Eldahan and Rabchevsky (2018) and other emerging strategies, but these interventions do not consider or treat the cause of AD, the noxious stimulus. Once the noxious stimulus is removed, BP goes back to normal and no drugs are required (Eldahan & Rabchevsky, 2018).

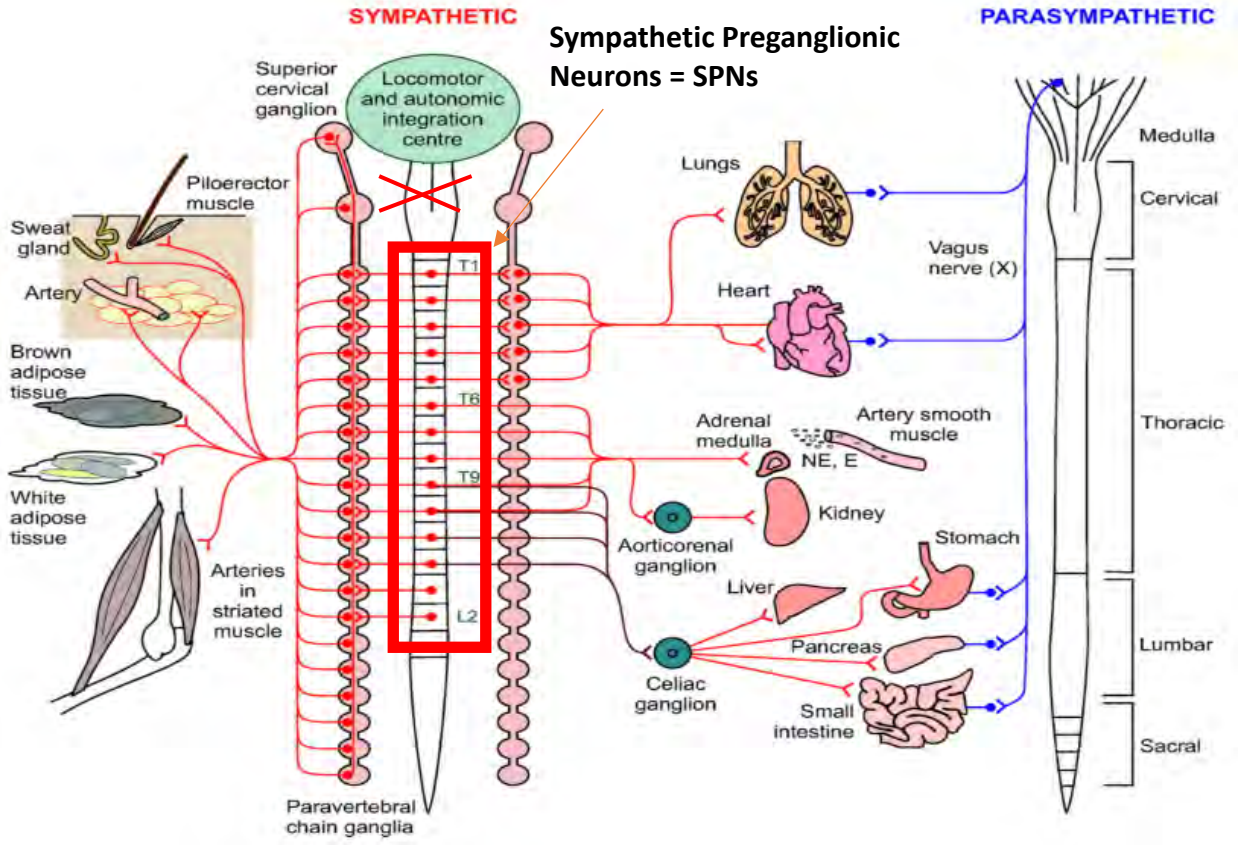


Modified from Cowley, 2018.

**Figure 3**: **Segmental organization of sympathetic preganglionic neurons in the sympathetic trunk and their target organ innervation**. T1-5 SPNs project to the heart and lungs, T6-T10 project to the adrenal medulla and aorticorenal ganglion, T9-T12 project to the liver, stomach, pancreas and small intestine. The parasympathetic system is located outside the spinal cord and innervates target organs in a segmental fashion. Following injury, descending drive from the autonomic integration centre is greatly reduced or absent.

## 2.3 Mesencephalic Locomotor Region (MLR)

Early work in the 1960s demonstrated that electrical stimulation of the MLR is capable of initiating locomotion. Increasing the intensity of stimulation increased both the speed and mode of locomotion, such that increasing intensity could increase not only speed, but convert walk to trot to gallop patterns of locomotor activity (Shik, Severin & Orlovsky, 1966). Subsequent electrophysiological and anatomical tracing experiments demonstrated that neurons arising from the MLR do not project directly to the spinal cord. Rather, reticulospinal (RS) neurons in the medulla (Noga, Kettler & Jordan, 1988) project from the MLR, through the ventrolateral funiculus (VLF) of the spinal cord and project to locomotor central pattern generator neurons under NMDA and non-NMDA control (Steeves & Jordan, 1980, 1984; Douglas et al., 1993). Cold block experiments in the medullary reticular formation (medRF) and VLF abolished locomotion induced by stimulating the MLR (Steeves & Jordan, 1984), demonstrating that the medRF is necessary for MLR evoked locomotion (Steeves & Jordan, 1984; Noga et al., 2003). Later work in the 1980s describes how the MLR, via extension of the medRF, could activate spinal central pattern generators involved in movement – when neurotransmitters were applied in the medRF, it was sufficient to induce locomotion (Steeves & Jordan, 1980, 1984; Shefchyk, Jell & Jordan, 1984; Noga, Kettler & Jordan, 1988, Noga et al., 2003).

## 2.4 Central Pattern Generators

Central pattern generators (CPGs) are neural networks able to generate rhythmic patterns of motor bursts which underly complex behaviours such as deglutition, mastication, respiration, and locomotion (Minassian et al., 2007; Steuer & Guertin, 2019). Locomotor CPGs receive

descending input from medRF reticulospinal neurons (RSNs) which receive input from the MLR and diencephalic locomotor regions (DLR; Grätsch, Büschges & Dubuc, 2019; Juvin et al., 2016; Jordan, 1998). Locomotor CPGs are found not only in cervical and lumbar enlargements, but throughout the spinal cord (Juvin, Simmers & Morin, 2005; Kiehn, 2006; Cowley & Schmidt, 1997; Kremer & Lev-Tov, 1997) and exist in lower vertebrates and as well as mammals (Minassian et al., 2007). The mammalian locomotor CPG is inherently more complex because it must coordinate the different muscles of the limb for associated balance reactions and further, coordinate four limbs to allow for walking, trotting and even galloping (Grillner & Kozlov, 2021).

Locomotor CPGs can generate basic locomotor rhythms in the absence of supraspinal or sensory information (Brown, 1911; Brown, 1914). Grillner and Kozlov's 2021 review summarizes what is known about the mammalian CPG and details the different conceptual models, such as the half-centre model (Grillner & Kozlov, 2021). The half-centre model was first proposed in 1914 (Brown, 1914) and McCrea, Rybak and colleagues have built on this model, suggesting that the locomotor CPG consists of two half-centre rhythm generators (McCrea & Rybak, 2008; Rybak et al., 2006) mediated by excitatory interneurons (INs) that reciprocally inhibit each other and directly excite antagonist groups of motoneurons and a pattern formation network (McCrea & Rybak, 2008; Rybak et al., 2006). These half-centres project and control flexor/extensor motoneurons, and this mutual inhibition between the half-centres is what allows only one half to be active at any given time. Phase switching occurs when the reduction of excitability from one half-centre falls below a critical value, and the other centre is released from inhibition (McCrea & Rybak, 2008). There is also indication that propriospinal coupling exists at

each segmental level between lumbar and cervical CPGs. Lumbar CPGs can drive cervical CPGs in the absence of pharmacologic activation at the level of the cervical spinal cord but cannot be activated in the opposite direction (Juvin, Simmers & Morin, 2005). Furthermore, Juvin and colleagues (2005) demonstrated that thoracic segments are constitutive elements of a distributed and rostrally projecting CPG network. Drug-activated caudal regions separated from rostral spinal regions were observed to be rhythmically active, demonstrating ascending lumbar influence on cervical CPGs as a function of the number of drug-exposed thoracic segments (Juvin, Simmers & Morin, 2005). This suggests locomotor output generated by lumbar CPGs can project to circuitry found in thoracic cord (Le Gal et al., 2016).

This half centre mediation of the locomotor CPG proposed by McCrea and Rybak is postulated to be regulated by ventrally derived spinal INs. INs are core elements of CPGs located within the ventral horn of the spinal cord (Kiehn & Kjaerulff, 1998) and ablating certain INs affects locomotor phenotypes (Ziskind-Conhaim & Hochman, 2017). Within the CPG, there are "core" interneurons (V0, V1, V2, V3) (Goulding, 2009; Stepien & Arber, 2008) based on distinct transcription factor expression, which are believed to mediate reciprocal inhibition and excitation between pattern formation and rhythm generation. Although there is significant understanding of the mammalian CPG, manipulation of whole classes of neurons has only become possible up until recently (Stepien & Arber, 2008).

## 2.5 Propriospinal Interneurons (INs)

Propriospinal INs originate and terminate within the spinal cord and span at least one spinal segment (Laliberte et al., 2019). Propriospinal INs are known for their heterogeneity (Jankowska, 2008) and Zholudeva and colleagues' review (2021) provides insight into IN

heterogeneity and their contribution to control of motor and sensory functions (Zholudeva et al., 2021). Propriospinal INs can have short or long ipsilateral or contralateral axonal projections, which can be ascending or descending, while some commissural INs have bifurcating projections with axon collaterals that ascend and descend within the spinal cord. Long propriospinal IN axonal projections give rise to ascending and descending pathways between cervical and lumbar enlargements, forming a major communication route between the two locomotors regions (English, Tigges & Lennard, 1985; Juvin, Simmers & Morin, 2005; Brockett et al., 2013; Laliberte et al., 2019). Cervical and lumbar enlargement connections project ipsilaterally and contralaterally and somas that give rise to them are mostly found in intermediate grey matter and lamina VIII, regions important for motor coordination (Brockett et al, 2013; Jankowska, 1992).

INs have been classified into “cardinal classes” based on distinct transcription factor expression, allowing us to visualize their projection patterns, migration patterns and understanding their roles in motor networks (Zholudeva et al., 2021; Goulding, 2009). Goulding’s review explains how neuronal identity is determined by morphogenic gradients in the spinal cord which subdivide into progenitor domains that give rise to different IN types (Goulding, 2009). In the ventral neural tube, there are four “core” classes of CPG INs (V0, V1, V2 and V3 INs) and motoneurons (Goulding, 2009). Within the putative core CPG INs, different subtypes also exist based on morphological and electrophysiological differences. V0 INs have contralateral rostral projections, extend 2-4 segments and ablation of V0 INs results in a hopping phenotype (Talpalar et al., 2013). V1 INs are inhibitory, have ipsilateral projections, project rostrally and V1 IN ablations show slower top speeds and prolonged flexion phases. V2 INs have local, ipsilateral projections and are subdivided into glutamatergic V2a and inhibitory V2b

neurons (Dougherty & Kiehn, 2010). V2a IN ablation causes variability in the amplitude and duration of locomotor cycles without affecting the frequency or pattern of coordination (Dougherty et al., 2013) whereas ablation of V2b INs causes hyperextension. Lack of both V1 and V2 INs results in complete loss of flexor-extensor alternation (Zhang et al., 2014). V3 INs are excitatory, have mainly contralateral rostral and caudal projections (Blacklaws et al., 2015) and V3 IN ablation results in less distinct patterns of left-right alternations (Zhang et al., 2008; Goulding, 2009; Laliberte et al., 2019). The table below summarizes the "core" CPG INs, the transcription factors they express, their neurotransmitter phenotype, their function/role in locomotion and their projection patterns (Goulding, 2009; Brownstone & Bui, 2010; **Table 1**).

Within the spinal cord, INs serve to coordinate activity with other spinal interneurons and motoneurons, making INs an attractive target for SCI therapeutics (Laliberte et al., 2019) as they can form "detour circuits" (Jankowska & Edgley, 2006) following SCI. Propriospinal INs are therefore ideal candidates for investigating their anatomical projections, since they relay ascending and descending motor commands within the spinal cord and are rhythmically active during locomotion (Cowley, Zaporozhets & Schmidt, 2010; Laliberte et al., 2019).

| Type | TF expression | Neurotransmitter | Function | Projections |
|---|---|---|---|---|
| $V0_D$ | Dbx1 (Pax7+) | Glycine/GABA | Left-right alternation (slow speeds) | -input to motoneurons |
| $V0_V$ | Dbx1 (Pax7-) | Glutamate | Left-right alternation (high speeds) | -input to motoneurons |
| $V0_C$ | Hb9, Isl1, Pitx2 | Acetylcholine | Motoneuron stability | -input to motoneurons |
| V1 | En1 | Glycine/GABA | Flexor/extensor alternation, regulate locomotor speeds | -input to motoneurons |
| Shox2 | Shox2+ | Glutamate | Rhythm generation | -input to motoneurons |
| V2a (shox2 +) | Chx10 | Glutamate | Left-right alternation | -ipsilateral input to motoneurons |
| V2b | Gata3 | Glycine/GABA | Flexor/extensor alternation | -input to motoneurons |
| V3 | Sim1 | Glutamate | Rhythm and gait stability | -input to contralateral motoneurons (primarily)<br>-input to other V3 INs |

**Table 1**: **Summary of different interneuron subtypes found in mouse spinal cord, their transcription factors, role in locomotion generation and their projections**.

* dorsal horn IN populations are also involved in sensory and pain processing (via Aβ fibre input; Duan et al., 2014; Tashima et al., 2021)

### 2.5.1 V3 Propriospinal Interneurons

V3 propriospinal INs are a defined class of INs marked by the transcription factor simpled-minded1 (Sim1, Blacklaws et al., 2015; Laliberte et al., 2019; Zhang et al., 2008), arising from the most ventral Nkx2.2+ p3 progenitor domain (Stepien & Arber, 2008). V3 INs are excitatory, have mostly contralateral projections and are essential for a stable and robust locomotor rhythm (Zhang et al., 2008; Borowska et al., 2015). Embryonic V3 INs assemble into distinct topographic clusters based on molecular transcription factors they express, resulting from combinations of different spatial and temporal differentiation patterns (Deska-Gauthier, Borowksa & Zhang, 2021). Morphologically, spatially, and functionally, V3 INs can be subdivided into different populations – dorsal, intermediate and ventral V3 IN subpopulations. V3 IN distribution has been mainly characterized for lower thoracic and upper lumbar segments because these regions are important for hindlimb movement (Borowska et al., 2013). Dorsal, intermediate and ventral V3 INs are observed in low thoracic and high lumbar regions whereas only intermediate and ventral V3 INs are found in the lower lumbar and sacral spinal cord (Borowska et al., 2013).

Dorsal V3 INs have greater initial processes, more complicated branching adjacent to soma and do not contact contralateral motoneurons whereas ventral V3 INs have fewer initial processes, are less branched, and their projections contact contralateral motoneurons (Borowska et al., 2013; Ziskind-Conhaim & Hochman, 2017). Dorsal and ventral V3 IN populations display differing electrophysiological patterns whereas intermediate V3 INs demonstrate “hybrid” properties of both the dorsal and ventral populations (Borowska et al., 2013 & 2015). Electrophysiologically, dorsal V3 INs have low gain with large afterhyperpolarization (AHP)

potential, large sag voltages and large post-inhibitory rebound potential, meaning they require more current to be excited based on their larger size. Whereas ventral V3 INs have high gain, tonically fire with 10 pA, have small AHP, small sag voltage and small post-inhibitory rebound potentials, meaning less current is required to be excited and are smaller in size (Borowska et al., 2013 & 2015). Ventral V3 INs can be further subdivided into V3 ventrolateral ($V3_{VLat}$) and V3 ventromedial ($V3_{VMed}$) IN populations due to their size, location and synaptic connectivity. Smaller $V3_{VMed}$ INs synapse with larger $V3_{VLat}$ INs that in turn, synapse with ipsilateral motoneurons (Chopek et al., 2018). **Figure 2a** is reflective of the difference in sizes seen between smaller $V3_{VMed}$ IN and larger $V3_{VLat}$ INs found in mouse spinal cord.

V3 INs are responsible for normal walking gait in adult mice, coordinate motor outputs from the left-right sides of the spinal cord, due to their mostly contralateral projections (>85%), (Chopek et al., 2018; Zhang et al., 2008; Stepien & Arber, 2008) and by controlling excitatory as well as inhibitory drives of the two sides of spinal cord (Goulding, 2009; Laliberte et al., 2019; Ziskind-Conhaim & Hochman, 2017). Inactivation of V3 INs in a Sim1-Cre mouse model that conditionally expresses tetanus light chain (TeNT), which blocks synaptic transmission through an allostatin receptor system reduces activity of V3 INs, resulting in disruption of the regularity of motor burst activity and variability in duration and step cycle period (Zhang et al., 2008; Stepien & Arber, 2008). Ventral V3 INs are recruited during swimming and running whereas dorsal V3 INs are only active during running as suggested by levels of c-Fos expression in these neurons (Borowska et al., 2013). This suggests that ventral V3 INs are involved in general locomotor activity output, synchronizing motor outputs across multiple levels (Laliberte et al., 2019), whereas dorsal V3 INs are recruited for running and weight bearing gaits and serve as

relay neurons that receive intense sensory inputs to adjust left-right coordination indirectly (Borowska et al., 2013; Laliberte et al., 2019). Ventral V3 IN axons extend mainly in caudal contralateral spinal regions whereas intermediate and dorsal V3 IN axons extend up to ~4200 µm rostral to L1 contralateral regions (Blacklaws et al., 2015). It is possible that V3 INs, which relay motor commands, are rhythmically active in locomotion and have long ascending projections within the spinal cord (Laliberte et al., 2019) could be mediating hypothesized connections between spinal locomotor neurons and SPNs (Cowley, 2018).

## 2.6 Epidural Stimulation (ES)

Clinically, facilitating locomotion on a voluntary basis would be more desirable than solely inducing locomotor-like movements, emphasizing the importance of understanding how ES can facilitate voluntary locomotion (Gerasimenko, Roy & Edgerton, 2008). ES has been shown to improve motor function after SCI in animal models and in humans below level of injury (Calvert et al., 2019). A device consisting of a series of electrodes is surgically implanted on top of the dura mater between the L1-L2 disc space (Legg Ditterline et al., 2020; Wagner et al., 2018). ES passes a current from a stimulator to large diameter dorsal root afferents, which activate motoneurons and lumbar interneurons to produce movements of the lower limbs (Minassian et al., 2007). Not only can ES restore voluntary movements below the level of injury, but it can also improve autonomic function, including improved cardiovascular responses, blood pressure (systolic over diastolic pressure), pulse pressure (systolic minus diastolic pressure) and temperature regulation (Cowley, 2018;  McKay et al., 2011a; McKay et al., 2011b; Legg Ditterline et al., 2020; Harkema et al., 2011; Flett, Garcia & Cowley, 2022). A recent review by Flett and colleagues (2022) summarizes all clinical trials to date that report improved autonomic

functions with either ES or transcutaneous stimulation (Flett, Garcia & Cowley, 2022). Neurons and neural pathways activated during ES are unknown, with large variability in results (Gerasimenko, Roy & Edgerton, 2008; Squair et al, 2021), sparking debate to ideal placement of electrodes and stimulation parameters (Calvert et al., 2019). It is postulated that improvements in cardiovascular parameters may be due to ES modulating efferent spinal sympathetic activity via INs involved in controlling posture and locomotion, due to proximity of these neural structures within spinal cord (Legg Ditterline et al., 2020).

## 2.7 Mouse Genetics

Sharif-Alhoseini and colleagues (2017) describe that for an injury or disease model to be reflective of a human condition it "should not only be similar in terms of the causation and function to the human analog but also must have advantages over simple clinical observation" (Sharif-Alhoseini et al., 2017). Mice and humans share similar genomes and using a mouse model for SCI has various advantages – they require relatively easy handling, are easy to generate knockout models in, and are highly reproducible (Sharif-Alhoseini et al., 2017). Various experiments investigating knockout (KO) models have allowed us to correlate different transcription factors (TFs) with different cell populations that may be involved different locomotor phenotypes they produce (Goulding, 2009). Taking advantage of mouse genetics to visualize specific propriospinal IN populations and developed genetic tools such as Cre-recombination, we can use our Sim1CreTdTomato mouse model to easily visualize V3 INs. Cre recombination is a powerful genetic tool used to understand biological processes and disease. Site specific gene recombination occurs when Cre recombinase recognizes loxP sites and cleaves the double-stranded DNA backbone, and depending on loxP site orientation, will invert or excise the flanked gene (Brown & Deiters, 2019). Sim1 is part of the basic helix-loop-helix-Per-Arnt-

Sim (bHLH/PSAS) family of TFs and is expressed in different regions of the central nervous system (CNS) in mice (Blacklaws et al., 2015). $Sim1^{Cre/+}$;tdTom mice can be generated, which endogenously express tdTomato in V3 INs which we will use to visualize V3 somas, axons and their projections.

## 2.8 Project Rationale

Descending drives are present in both locomotor propriospinal networks and in sympathetic function, and since sympathetic function increases with overground locomotion or exercise, it is likely there may be connectivity between the two systems. Integration between locomotor and sympathetic centres is observed in the brainstem, but this communication is lost after injury. However, there have been instances in which ascending control from lumbar spinal segments can coordinate and integrate movement without brainstem spinal centres (Juvin, Simmers & Morin, 2005). Few studies have examined the target projections of propriospinal neurons (Brockett et al., 2013), let alone the characterization of integration between spinal neurons or circuits responsible for locomotor and sympathetic integration (Cowley, 2018) in the ascending direction. We hypothesize that propriospinal interneurons, which relay motor commands, are rhythmically active in locomotion and have long ascending projections within the spinal cord (Laliberte et al., 2019) could coordinate activity between spinal locomotor centres and SPNs.

By understanding if propriospinal INs in specific lumbar segments project to thoracic SPNs, this will provide insight into the optimal placement of epidural stimulators to activate lumbar motor networks but also, to help optimize stimulation locations that could simultaneously activate locomotion and sympathetic circuitry. This project will provide novel insight into the

distribution and pattern of input from lumbar locomotor related neurons onto thoracic SPNs to understand underlying complexities within the spinal cord. No examination of integration of spinal locomotor circuitry and spinal sympathetic neurons has been conducted; therefore, this study will be the first characterization of lumbar locomotor-related IN projections to SPNs and if they are indeed involved in sympathetic activation.

## 2.9 Hypotheses & Aims

### 2.9.1 Overarching Hypothesis:

*Lumbar V3 INs in lumbar regions synapse on thoracic SPN neurons, and a higher density of contacts is present in more rostral thoracic regions.*

### 2.9.2 Specific Aims & Aim Hypotheses

1) Determine if V3 INs synapse on thoracic SPNs.
    a. **Hypothesis 1**: Lumbar *V3 INs innervate thoracic SPNs.*
2) Determine if V3 INs in specific lumbar segments project to SPNs in specific thoracic regions.
    a. **Hypothesis 2**: V3 INs located in rostral lumbar segments project to *and have higher numbers of synaptic contacts on thoracic SPNs compared to V3 INs located in caudal lumbar segments.*
3) Characterize the distribution patterns of lumbar V3 IN projections to thoracic SPNs.
    a. **Hypothesis 3**: *There is greater density of synaptic contacts in the upper thoracic region from lumbar V3 INs compared to lower thoracic segments*.

# Chapter III: Methods

## 3.1 Ethics Declaration

All procedures were approved by the University of Manitoba Central Animal Care Committee (protocol 20-056) prior to commencement of experiments and were performed in accordance with the guidelines set forth by the Canadian Council on the Animal Care Committee.

## 3.2 Animals & Mouse Genetics

Generation and genotyping of $Sim1^{Cre/+}$ mice we performed as previously described by Zhang and colleagues (2008) (Zhang et al, 2008). $Sim1^{Cre/+}$ mice were then subsequently crossed with TdTomato Ai9 mice ($Rosa26^{floxstopTdTom}$, Jackson Laboratory) to generate Sim1Cre-tdTomato mice which endogenously express the fluorescent protein tdTomato in their somas, axons and axon terminals. Adult male and female Sim1Cre-tdTomato mice were used in this series of experiments.

## 3.3 Experimental Design

### 3.3.1 Defining anterograde and retrograde tracers

Tracers are defined as retro- or antero-grade based on their direction of travel within neurons. Retrograde tracers are taken up by terminals at injection site and travel back via axons to cell bodies, whereas anterograde tracers are taken up by cell bodies and travel via axons to terminal processes. Cholera toxin subunit B, a reliable retrograde tracer has been commercially used since 1977, with new fluorescent probes attached for ease of visualization. Dextran amines emerged in the 1980s and are conventionally used as anterograde tracers (Saleeba et al., 2019).

### 3.3.2 Biotin-dextran Amine (BDA) Tracer

Biotin-dextran amine (BDA) is a powerful tracer due to its ability to trace nerve pathways for neuroanatomical labelling studies and are used to map neuronal connectivity (Lazarov, 2013). High molecular weight BDA-10,000 (10 kDa BDA) seems to preferentially be transported anterogradely (Reiner et al., 2000), able to label axons and their terminals (Lazarov, 2013). BDA enters through injured neurons at the site of injection and spreads anterogradely through diffusion, resulting in Golgi-like staining (Saleeba et al., 2019). Due to its molecular weight, we pipetted BDA right before performing injections to prevent it from blocking the ~120 um glass electrode tip.

### 3.3.3 Cholera Toxin Subunit B (CTB) Tracer

Cholera toxin subunit B (CTB) is a homopentameric protein that is roughly 55 kDa (Baldauf et al., 2015) and was first introduced as a retrograde tracer in 1977 (Stoeckel, Schwab & Thoenen, 1977). The development of Alexa Fluor (AF) conjugates of CTB have extended the scope of CTB neuroanatomical tracing leading to brighter and photostable results. CTB binds to cell surfaces via its receptor monosialoganglioside (GM1) and enters axons or dendrites via nerve terminals or through damaged axons (Lai et al., 2015). CTB receptor mediated internalization is transported to trans-most cisterns and tubules of the Golgi apparatus and lysosomes in somas. Transported CTB remains in vesicles, which may explain why it produces granular appearances of label in somas but is less evident in neuronal processes (Lai et al., 2015; Conte, Kamishina & Reep, 2009; Dederen, Gribnau & Curfs, 1994; Saleeba et al., 2019). Since CTB is a large molecule, it has increased viscosity and to prevent air bubbles forming inside

syringes or CTB from occluding the micropipette, a minimum of 5 µL of tracer was pulled into the glass micropipette.

### 3.3.4 Surgical Procedures

Prior to surgery, mice were handled daily to acclimate them to necessary handling during recovery. Water gel, fruit treats, bacon treats and Clear H2O®DietGel®Boost Purified High Calorie Dietary Supplement were placed on the floor of their home cages in case mobility was affected post-surgery. Pre-operative weights were obtained and mice were prepared for aseptic surgery. Mice were induced with 4% isoflurane with a flow rate of ~ 2 L of oxygen and maintained with ~2% isoflurane with a flow rate of ~0.8 L of oxygen. Eye lube was placed on eyes to prevent drying out, backs of mice were shaved and washed three times with soap and ethanol, and hindlimb nails were trimmed. Mice then received subcutaneous injections of meloxicam (2 mg/kg) in 1 ml of saline, then transferred to the surgical suite where they underwent spinal cord stereotaxic injections.

### 3.3.5 Stereotaxic Injections

Absence of a pedal reflex was indicative of an appropriate plane of anaesthesia for injections. Body temperature was maintained at 37 °C through rectal temperature probe monitoring and an electric heat pad. Mice were placed in a stereotaxic frame; back muscles were dissected to expose 2 to 3 vertebrae and a laminectomy was performed. Spinal segment landmarks were visualized and referenced (Harrison et al., 2013) to identify where biotin-dextran amine (BDA-10,000) would be pressure injected along the lumbar (L1-L5) segments of the spinal cord. Using a stereotaxic micromanipulator, a 75 RN SYR 5 µL Hamilton Syringe

(Hamilton) was placed over the lumbar region of the spinal cord. Between 0.5-1 µL of BDA (Thermo Fisher Scientific Cat# D1956, RRID:AB_2307337) was injected, using a motorized pico-injector, with Hamilton syringes fitted with a single-barrel borosilicate capillary glass with microfilament (A-M Systems Inc.) pulled to a ~120 µm tip over five minutes into the spinal cord (700-1000 µm down). After the initial five minute of injection time, the pipette remained in spinal cord for five minutes before withdrawal to prevent BDA drawback into the tip and ensure full delivery of BDA. Skin was then sutured (Ethicon 5-0 Coated VICRYL Plus Antibacterial (Polyglactin 910 Suture) and sealed with Vetbond to prevent opening of the incision. Mice were then given slow-release buprenorphine (0.5 mg/kg) and glucose (0.02 ml/g) post-operatively. Once mice recovered from anaesthesia, they were placed back in their home cages. The following day, Meloxicam analgesic was administered (s.q. 2 mg/kg in 1 ml of saline) and received post-operative monitoring and care for one week. Hibitane antibacterial ointment was applied to incision site as necessary and Tobrex was applied if eyes appeared dry post-surgery. If any dehydration occurred, 5% dextrose in saline was injected subcutaneously as needed. See post-operative monitoring sheet in **Appendix (pg. 90-91).**

In a sub-set of mice, under same conditions above, injections in thoracic spinal cord (~T8) with Cholera toxin B Alexa 488 (CTB-A488) were done to investigate which populations of lumbar V3 INs project to thoracic SPNs. CTB-A488 injected volumes ranged between 0.5-1 µL and were all injected over 7 minutes with rest of 5 minutes before removing the glass capillary tip.

### 3.3.6 Spinal Cord Harvesting & Sectioning

One-week post-surgery, mice were deeply anaesthetized with isoflurane and trans-cardially perfused with 20-30 mL of 1x Phosphate-buffered saline (PBS) followed by 20-30 mL of 4% paraformaldehyde diluted down from 16% paraformaldehyde (PFA; Alfa Aesar) in PBS. Spinal cords were then excised from body and placed overnight in 4% PFA solution. The following day, spinal cords were washed three times for ten minutes in 1x PBS before being cryoprotected in 30% sucrose (Fisher Scientific) in PBS.

Spinal cord dura were removed and spinal cords were blocked into cervical, thoracic and lumbar segments. Tissue was frozen in Tissue-Tek® O.C.T Compound (Sakura) and cryosectioned at 18 µm and 30 µm (CryoStar NX50 ThermoScientific) for thoracic spinal cords in BDA injected mice and remainder of blocked spinal cords, respectively. Sections were mounted on Precleaned Superfrost Plus Microscope Slides (Fisherbrand) and stored at -20˚C.

### 3.3.7 Immunohistochemistry

Immunohistochemistry (IHC) is used to visualize proteins or cells of interest. Some IHC protocols required the use of antigen retrieval prior to addition of primary antibodies to enhance visualization of antibody of interest, and in our case, ChAT which labels cholinergic SPNs. Although formaldehyde is commonly used as a preservative, it can result in “masking” of antigens (Leong & Leong, 2007). Amino acid side chains of proteins can react with aldehydes to stabilize proteins, and this is believed to “mask” epitopes of different antigens and disrupts hydrogen bonds which can also alter epitopic targets (Leong & Leong, 2007). Antigen retrieval using Tris-EDTA buffer at 55˚C for 10 minutes provides sufficient heat to break cross-links

formed by formalin fixation (Leong & Leong, 2007), resulting in better penetration of antibodies into tissue, especially when using ChAT antibody.

VGlut1 and VGlut2 specifically label glutamatergic neurons in the CNS and allow them to be reliable markers for glutamatergic neurons, as opposed to glutamate which can be co-express in GABAergic neurons (Zhang et al., 2018). For this reason, we used VGlut2, a presynaptic marker known to be expressed in glutamatergic spinal cord interneurons (Moechars et al., 2006). ChAT enzyme catalyzes the synthesis of acetylcholine neurotransmitter which is responsible for regulating signal transduction at the neuromuscular junction. Since SPNs are cholinergic, we used ChAT to stain for SPNs and identify them based on their location in the spinal cord (IML; Witzemann, 2007). DsRED antibody was used to recognize our fluorescent protein of interest in V3 INs that endogenously express the fluorescent protein, tdTomato (Chopek et al 2018).

**BDA, ChAT, tdTomato:** Slides were warmed to room temperature (RT) washed 3x 10 minutes in PBS-T (0.2%), followed by antigen retrieval (10-minute incubation at 55 $^{\circ}$C in Tris-EDTA buffer), washed again 3x 10 minutes in PBS-T (0.2%) and then placed in a 10% normal donkey serum block in PBS-T (0.2%) for one hour. Primary antibodies dsRED (1:1000) and ChAT (1:400) were applied to slide and left for 72 hrs at 4 $^{\circ}$C to aide in ChAT antibody penetration. After which, slides were washed 3x 10 minutes in PBS-T (0.2%) followed by secondary antibodies Streptavidin647 (1:500), Alexa488 (1:250) and Cy3 (1:500, 1:1 glycerol) for two hours in the dark at RT. Slides were then washed 1x 10 minutes in PBS-T (0.2%)

followed by 2x 10 minute washes in Tris-HCl 50Mm then dried and cover-slipped in BioLynx VECTASHIELD HardSet Mounting Medium (Vector Laboratories).

**VGlut2, ChAT, tdTomato**: The same protocol was used as above for antigen retrieval and slides were incubated with primary antibodies dsRED (1:1000), VGlut2 (1:500) and ChAT (1:400). After 72 hours of incubation, slides were washed 3x 10 minutes in PBS-T (0.2%) before being placed in secondary antibodies Cy3 (1:500, 1:1 glycerol), Alexa647 (1:500, 1:1 glycerol) and Alexa488 (1:250) respectively for two hours in the dark at RT. Same procedures were used to wash off secondary antibodies and for storage of slides as listed above.

| **Primaries** | **Concentration** |
|---|---|
| dsRed | 1:1000 |
| VGlut2 | 1:500 |
| ChAT | 1:400 |
| BDA | Injected (~1 µL) |
| CTBA488 | Injected (~1 µL) |
| **Secondaries** | **Concentration** |
| Cy3 α rabbit (1:1 glycerol) | 1:500 |
| Alexa 488 | 1:250 |
| Alexa 647 (1:1 glycerol) | 1:500 |
| Streptavidin Alexa Fluor 647 | 1:500 |
| Streptavidin Alexa Fluor 488 | 1:500 |

**Table 2: List of antibodies used for IHC protocols and their concentrations.**

### 3.3.8 Microscopy & Image Analysis

Images were obtained on a Zeiss Axio Imager Z.2 upright microscope or on a Zeiss LSM 880 with Airyscan confocal microscope. Injection sites and double labelled CTB-$A488^{+}$/$tdTomato^{+}$ cells were counted on the Axio Imager. Thoracic IML SPNs were imaged at 63x magnification (between ~8-12 Z-stacks per image) at 1x zoom on the confocal microscope to be imported into IMARIS Bitplane software for 3D reconstruction and analysis. Laser settings were optimized and retained to ensure consistent imaging parameters were used for each slide. ~15-20 IML SPN slices per T1-T6 and T7-12 were imaged and analyzed to obtain a representative rostro-caudal distribution of IML SPNs per mouse (n = 4 mice). Left and right IML SPNs were imaged and selected based on visibility of at least one SPN soma. IMARIS "Surface" tool was used to reconstruct somas of SPNs. "Surfaces" were also used to reconstruct puncta for V3 axon projections, BDA and VGlut2. Machine learning (ML) trained the program to distinguish true contacts (Class A) from noise (Class B) for V3 puncta, BDA or VGlut2 by implementing 3-4 levels of ML to optimize parameters. Filters were set for VGlut2 to detect Class A puncta that were less than 1 µm from SPN somas (set at 1) and V3 puncta had to be at overlapped with VGlut2 to be counted as double labelled $VGlut2^{+}$/$tdTomato^{+}$ (set at 0). $TdTom^{+}$/$VGlut2^{+}$ and $BDA^{+}$/$tdTom^{+}$ puncta surface area ratios were also calculated by selecting 10 SPN cells (either fusiform or round cell types) in both T1-T6 and T7-T12 segments (# of puncta/100 $\mu m^2$).

To examine V3 terminal density in thoracic IML, the right half of grey matter of thoracic spinal cord was imaged using a 20x objective lens, 2-3 Z-stacks, and the tiling function on Zeiss ZEN Black software (1 horizontal x 3 vertical tiles, 2 horizontal x 2 vertical or 2 horizontal x 3

vertical tiles to capture entirety of right-side grey matter), depending on orientation of spinal cord section. One image was taken per spinal segment to obtain representative V3 puncta organizations within the IML (12 images per mouse, n = 3 mice). Images were then stitched in IMARIS Stitcher and analyzed in IMARIS. “Spots” detection method was used to select V3 puncta on right side of spinal cord and V3 puncta were classified into Class A (true puncta) and Class B (noise/not true puncta), and XY coordinates of Class A V3 puncta from grey matter were exported from IMARIS and transformed into scatter and contour plots in RAWGraphs (https://app.rawgraphs.io/). A region of interest (ROI) set in IMARIS around the IML (dimensions X: 400 Y: 395) was used to analyze differences of V3 IN puncta density in this region at different thoracic segment levels throughout the spinal cord. The quantity of Class A puncta were exported from IMARIS and statistically analyzed in GraphPad Prism.

V3 IN somas were counted on a Zeiss Axioscop 40 and every 3$^{rd}$ (every ~450 µm) slice per slide was counted to obtain a representative number of V3 somas found throughout the thoracic and upper lumbar spinal cord (n = 5 mice).

CTB-A488$^{+}$/tdTomato$^{+}$ somas in lumbar spinal cord were counted by creating tiled, Z-stack images at 10x magnification on a Zeiss Axio Imager Z.2 upright microscope and counted in ZenLite software. ~10 sections from L1-L6 were imaged per mouse (n = 4 mice). Sections were then divided into either dorsal, intermediate or ventral quadrants of the left and right sides of the spinal cord to compare double labelled somas on the ipsi- and contra-lateral sides of injection site and to investigate which neuronal populations may be projecting to IML. Neurons that were extremely out of focus in the maximum intensity projection (MIP) images were

excluded, and to be considered double labelled, there had to be either a distinguishable outline of neuronal shape with CTB and or had to have perinuclear labelling with 4-5 distinct vesicle speckles within demarcations of soma (Conte, Kamishina & Reep, 2009).

### 3.3.9 Statistical Analysis

GraphPad Prism software was used to perform one-way ANOVA and multiple comparisons tests on T1-T6 and T7-12 groups to analyze differences in $VGlut2^{+}$/$tdTomato^{+}$ and $BDA^{+}$/$tdTomato^{+}$, puncta-surface area ratios, differences in V3 soma counts in T1-T6, T7-T12 and L1-L2 regions of the spinal cord, when comparing $CTBA488^{+}$/$tdTomato^{+}$ somas in lumbar regions of thoracically injected CTB-A488 mice, and when analyzing IML ROI V3 puncta quantities.

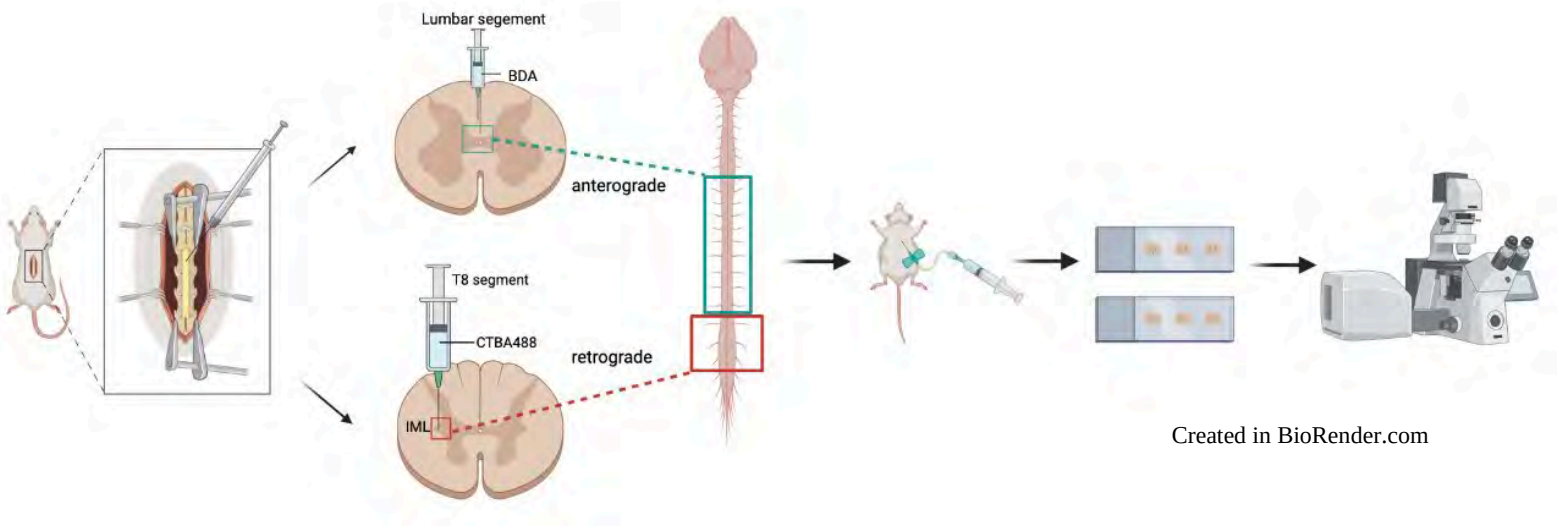


**Figure 4: Summary of experimental procedures detailing stereotaxic surgery, tracer injections, spinal cord harvesting, sectioning and imaging.**

# Chapter IV: Results

## 4.1 Distribution of V3 INs within the thoraco-lumbar spinal cord

*Greater number of V3 INs observed in lumbar versus thoracic spinal cord*

V3 INs have been analyzed in low thoracic and upper lumbar spinal cord mainly because this region is involved in hindlimb locomotion, however their distribution in thoracic spinal cord has not been investigated (Borowksa et al., 2013; Blacklaws et al., 2015). We observed V3 somas throughout the entire thoracic spinal cord and observed sparse, smaller dorsal and ventral V3 somas in T1-T6 and T7-12 regions (mean =16.6 somas, n = 70 cells, and 14.0 somas n = 69 cells, respectively, from 5 mice total). One-way ANOVA and Tukey's multiple comparisons test revealed that the number of V3 IN somas was significantly higher in upper lumbar segments L1-L2 (mean = 32.85 somas, n = 54 cells), compared to T1-T6 and T7-T12 regions, where large dorsal and ventral V3 IN populations could be observed (*$p<0.05$, ****$p< 0.0001$, n = 5 mice, **Figure 5**). Although sparse V3 somas can be found throughout thoracic spinal cord, this data suggests that most V3 IN axon projections are lumbar in origin and have long ascending projections.

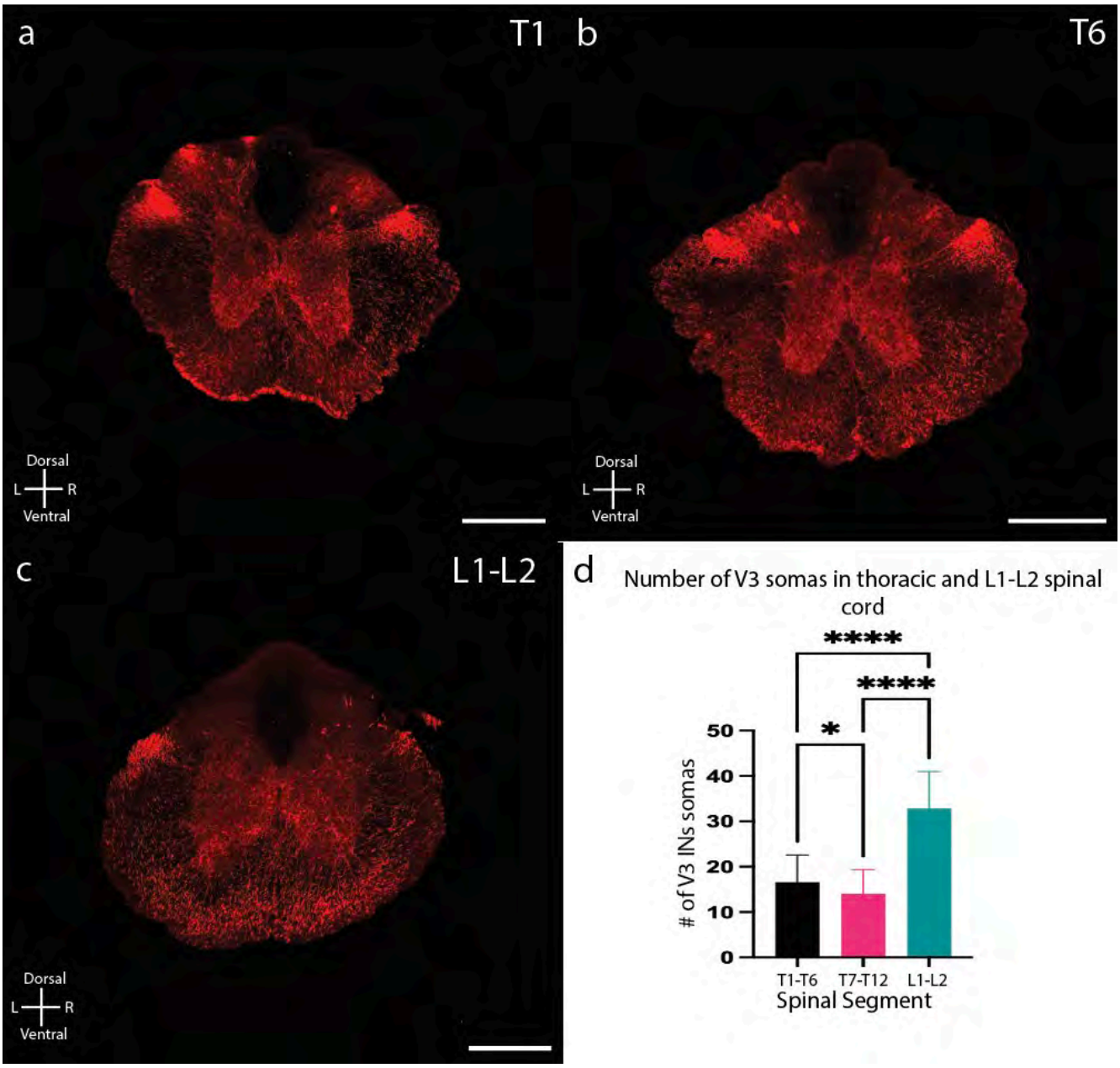


**Figure 5: Greater number of V3 somas in lumbar vs. thoracic spinal cord.** a-b) Sparse and small ventral and dorsal V3 somas observed in thoracic spinal cord c) Numerous ventral and dorsal V3 INs observed in upper lumbar region of spinal cord d) Bar graph of mean number of V3 somas observed throughout T1-T6, T7-T12 and L1-L2 spinal cord (mean = 16.6, 14.0 and 32.85 somas respectively, n = 70, 69, 54 cells respectively) with SD (one-way ANOVA and Tukey's multiple comparisons tests, * $p < 0.05$, **** $p < 0.0001$, n = 5 mice total, **Scale** = 500 µm).

*Large V3 IN puncta density near IML in thoracic spinal cord*

Based on initial visual observations that V3 INs have puncta near the IML (**Figure 6a**), we sought to quantify puncta densities in this region. IMARIS analyzed puncta XY coordinates were imported into RAWGraphs to generate representative heat maps of V3 puncta in grey matter of spinal cord in T1-T12 (**Figure 6b**). Heat maps show relative concentrations of data groupings by colour coding them based the number of marks in the group, where red represents high concentrations and blue represents low concentrations. Puncta density in three mice ranged between ~1000-1500 puncta in T1-3 segments, increased to a peak of ~1400-2500 puncta in T4/T5 segments with puncta decreasing to ~1200 puncta in T6/T7 segments, and down to ~500-1000 throughout the remaining caudal thoracic segments (**Figure 6c**). No V3 somas were observed in any IML ROIs. Noble et al., (2022) and Ueno et al., (2016) demonstrate excitatory input to thoracic SPNs, but the source of the input is unknown (Ueno et al., 2016; Noble et al., 2022). As described previously, V3 INs are excitatory and glutamatergic (Zhang et al., 2008), and the high prevalence of V3 puncta within the IML we show here, suggests they may appose and provide excitatory input to SPNs of the IML.

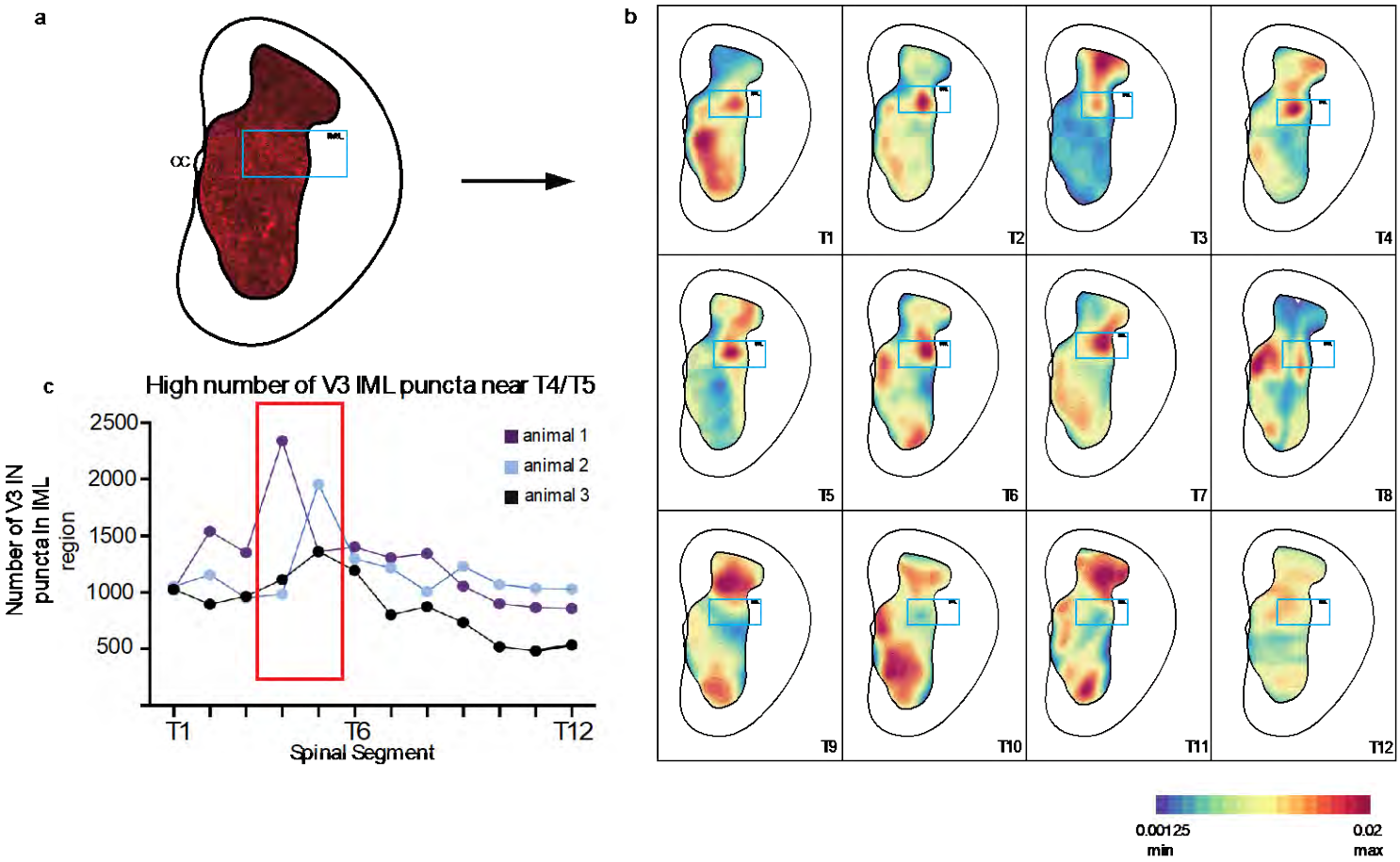


**Figure 6**: **High number of puncta observed near IML in thoracic spinal cord**. a) Representative right half section of grey matter of thoracic spinal cord with IML ROI in blue box. Images are analyzed in IMARIS where XY coordinates of V3 puncta are exported to RAWGraphs and transformed to b) representative heat maps of each thoracic segment (Blue = minimum intensity, Red = maximum intensity) c) IMARIS quantification of V3 puncta in IML ROI show peak in number of puncta near T4-T5 region (n = 3 mice).

*V3 IN presynaptic terminals appose SPNs throughout thoracic spinal cord*

As we demonstrated high concentration of putative V3 puncta within the IML, we performed immunohistochemical analysis to confirm whether these putative contacts are indeed presynaptic V3 IN terminals in the IML. Using the presynaptic terminal marker VGlut2, and DsRED to label V3 IN terminals, we confirmed that V3 INs indeed appose SPNs throughout thoracic spinal cord (**Figure 7Ai-Aiv & Bi-iv**). 3D reconstructed IMARIS Bitplane images of T1-T6 and T7-T12 SPNs, VGlut2 and V3 IN puncta allowed us to quantify $VGlut2^{+}/tdTom^{+}$ puncta (**Figure 7Ci-Cii**). Out of all VGlut2 innervation on thoracic SPNs, ~20% of these connections originate from V3 INs (**Figure 7D**, confirmed by $VGlut2^{+}/tdTom^{+}$).

We hypothesized there would be a greater number of V3 contacts on rostral (T1-T6) segments on the assumption these segments are responsible for heart innervation. However, we found no significant differences in percentage of double labelled $VGlut2^{+}/tdTom^{+}$ contacts in T1-T6 compared to T7-T12 (**Figure 7D**, $p > 0.345$, $n = 4$ mice). Based on our method of separating the thoracic spinal cord into rostral (T1-T6) and caudal (T7-T12) segments, this did not allow us to detect a significant difference in proportion of contacts even though we observed a peak at T4/T5. This suggests that the proportion of contacts may vary by segment and future experiments should be designed to examine and answer this question.

Due to variability in the number of SPNs in analyzed in each image in IMARIS , we also investigated reconstructions of individual 3D $VGlut2^{+}/tdTom^{+}$ puncta size to SPN surface area (SA; $\frac{\#\ \text{VGlut2+/tdTom+}\ puncta}{per\ 100\ \mu m\text{^}2}$) for 10 SPNs each in T1-T6 and T7-T12 according to methods described by Smith and colleagues (Smith et al., 2017). The mean puncta to SA ratio was 0.63

and 0.64 for T1-T6 and T7-T12, respectively, and found no significant differences were found (n = 40 cells, $p > 0.988$, unpaired t-test, 4 mice). Again, based on the observed peak of puncta at T4/T5, it cannot be fully concluded that there is even $VGlut2^{+}/tdTom^{+}$ distribution throughout thoracic spinal cord.

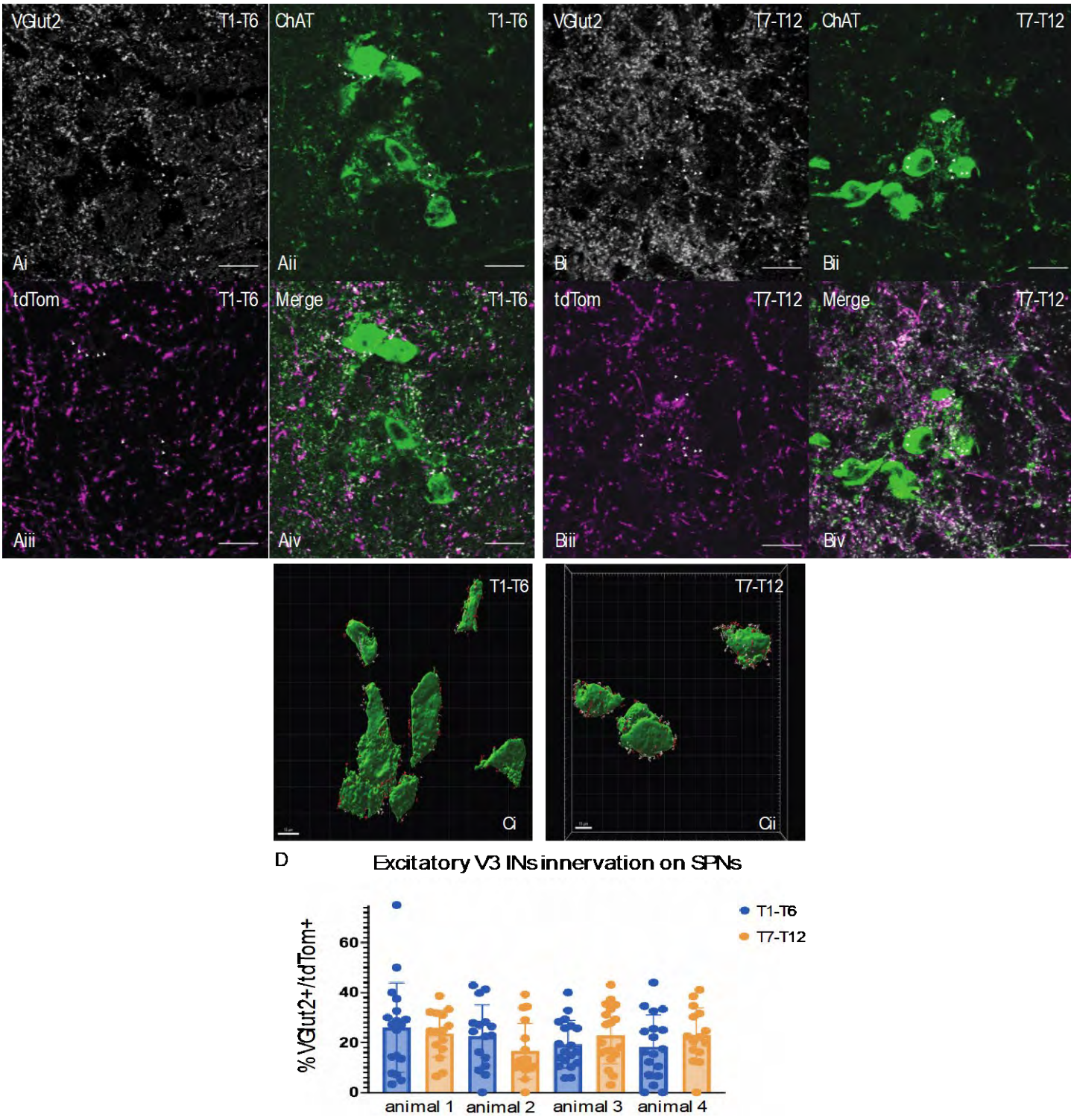


**Figure 7**: **~20% of all VGlut2 innervation on SPNs originate from V3 INs**. Ai-iv & Bi-iv) Co-localized VGlut2 and V3 IN puncta on SPNs in T1-T6 and T7-12 spinal cord indicated by arrow heads. (**Scale** = 20 μm). Ci-ii) 3D reconstructed IMARIS Bitplane image of T1-T6 and T7-T12 SPNs, VGlut2 and V3 puncta (**Scale** = 10 μm) D) Percentage of $VGlut2^{+}/tdTom^{+}$ contacts on SPNs in different mice with no significant difference between T1-T6 and T7-T12

spinal segments (one-way ANOVA and Tukey's multiple comparison tests, $p > 0.3453$, $n = 4$ mice).

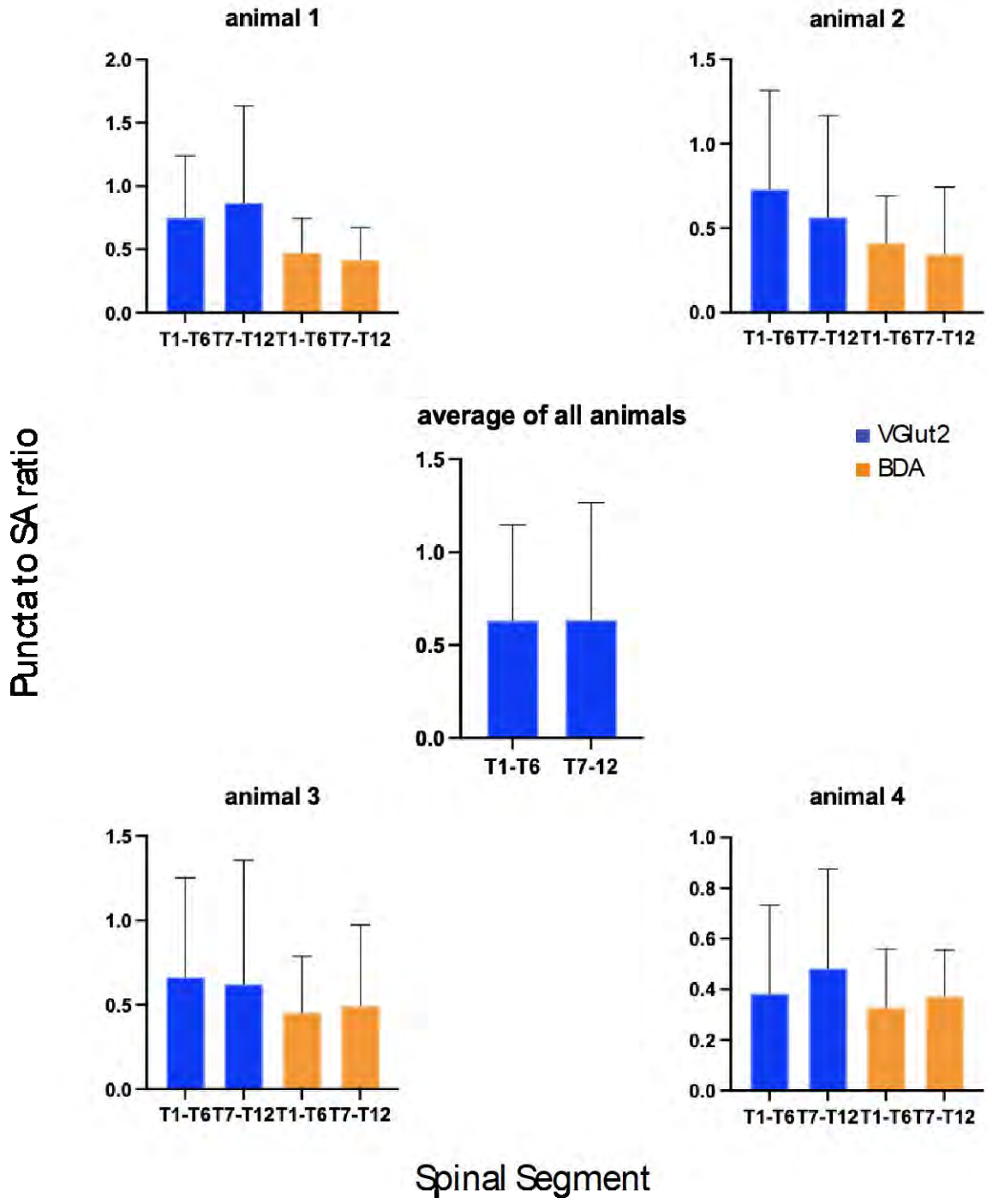


**Figure 8**: **Puncta to SA ratios for VGlut2$^+$/tdTom$^+$ and BDA$^+$/tdTom$^+$ on SPNs**. No significant differences observed between T1-T6 and T7-T12 VGlut2$^+$/tdTom$^+$ ratios (**n = 4 mice**). Average ratios of all mice for VGlut2$^+$/tdTom$^+$ puncta also did not show significant differences (mean = 0.63 and 0.64 for T1-T6 and T7-T12 respectively, n = 40 cells, p > 0.9880, unpaired t-test, 4 mice). BDA$^+$/tdTom$^+$ puncta to SA ratios were also insignificant but had

higher puncta ratios for either T1-T6 or T7-T12 depending on injection site (mouse 1 & 2 = L2 injections, mouse 3 = L3 injection, mouse 4 = L4/L5 injection). In L2 injected mice, puncta to SA ratios were higher in T1-T6 compared to T7-T12 (mean 0.45 vs. 0.38 respectively, n = 10 cells, 2 mice), L3 injected mice had higher puncta to SA ratio in T7-T12 compared to T1-T6 (mean 0.50 vs. 0.46 respectively, n = 10 cells, 1 mouse) and L4-L5 injected mice had higher puncta to SA ratio in T7-T12 versus T1-T6 (mean 0.37 vs 0.33 respectively, n = 10 cells, 1 mouse).

## 4.2 Projections of V3 INs

*Lumbar V3 INs show distinct thoracic SPN projection profiles, revealed by segmental level of BDA injection site*

We performed BDA injections at different lumbar segments to investigate whether differences exist in the rostrocaudal distribution of V3 IN projections from rostral versus caudal lumbar regions (**Figure 9**). While no significant differences were observed in total VGlut2$^+$/tdTom$^+$ labelling between T1-6 and T7-T12 segments, we did, observe differences in BDA$^+$/tdTom$^+$ labelled projections (**Figure 10Ai-iv, 10Bi-iv & 10Ci-ii**) depending on injection level.

Mice injected at L2 showed a significantly higher percentage of BDA$^+$/tdTom$^+$ puncta in T1-T6 compared to T7-T12 (**$p<0.0067$, n = 2 mice). Mice injected at L3 showed no significant difference in percentage of BDA$^+$/tdTom$^+$ puncta between T1-T6 and T7-12 (n = 1 mouse), and mice injected at L4-L5 had significantly more BDA$^+$/tdTom$^+$ puncta in T7-T12 (***$p<0.0004$, n = 1 mouse) compared to T1-T6 (**Figure 10D**, n = 4 mice total).

In terms of puncta to SA ratios within T1-T6 and T7-T12 regions, no significant differences were observed in the 4 mice analyzed. However, it was observed that BDA injections at L3 showed higher puncta ratios in T1-T6 compared to T7-T12 (mean 0.45 vs. 0.38 respectively, n = 10 cells, 2 mice), injections at L3 showed higher puncta to SA ratio in T7-T12 compared to T1-T6 (mean 0.50 vs. 0.46 respectively, n = 10 cells, 1 mice) and injections at L4-L5 showed higher puncta to SA ratio in T7-T12 versus T1-T6 (mean 0.37 vs 0.33 respectively, n = 10 cells, 1 mice). Altogether, this suggests that projections of lumbar V3 INs have distinct

rostrocaudal distribution patterns depending on the lumbar location of V3 INs. L2 V3 INs preferentially project to T1-T6 SPNs compared to L4-5 V3 INs that preferentially project to T7-T12 SPNs. This distribution may be important when it comes to modulating sympathetic activity since rostral segments of the locomotor CPG seem to have a more “rhythmogenic” capacity (Kiehn, 2006; Cowley & Schmidt, 1997; Kremer & Lev-Tov, 1997), and could be why rostral lumbar V3 INs favour projecting to T1-T6, to modulate sympathetic activity of the heart.

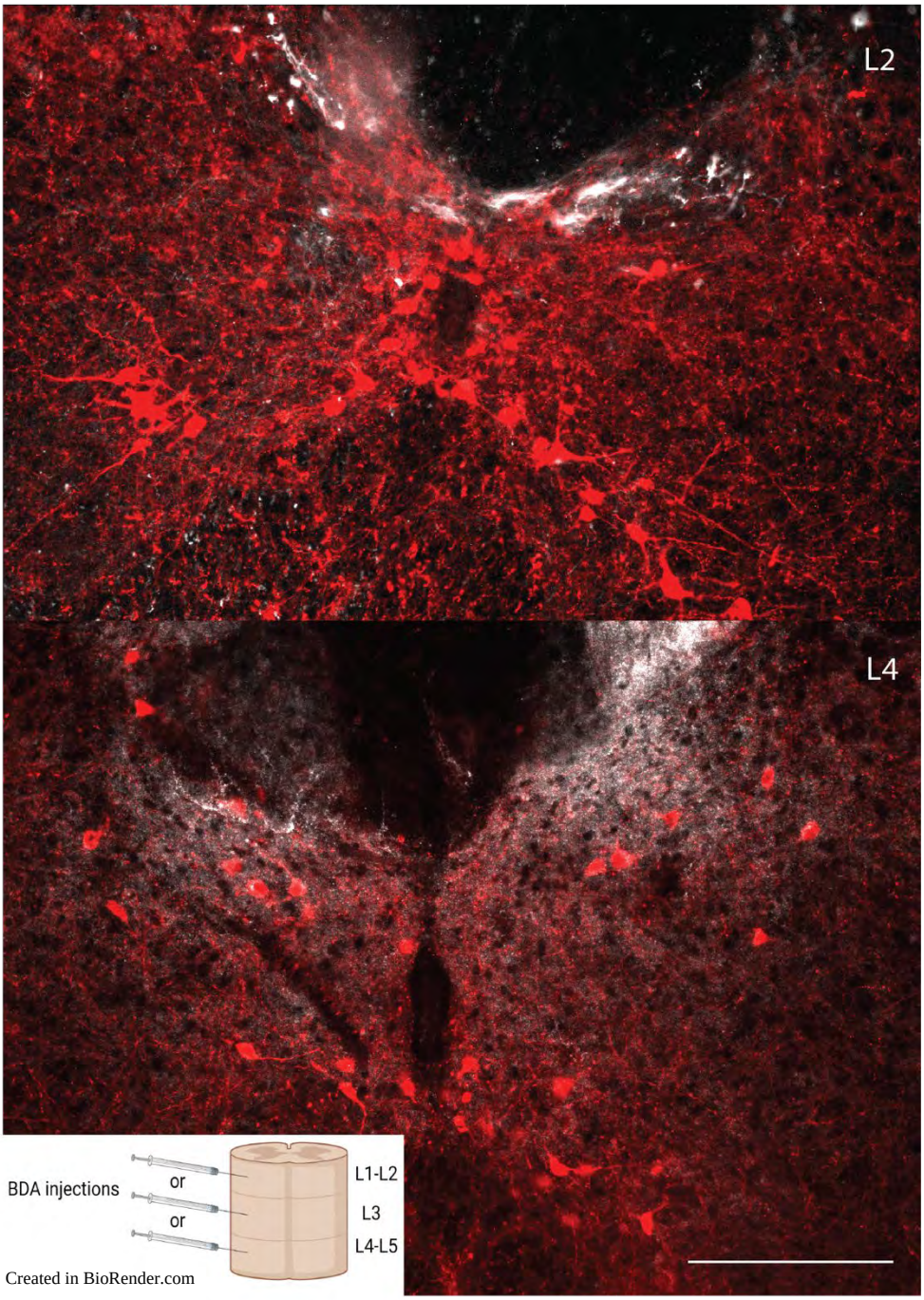


**Figure 9**: **Summary of surgical procedure for BDA injections**. Injection sites into L2 and L4 spinal cord. BDA tracer (white) and Sim1CreTdTomato V3 INs (red). **Scale** = 200 µm.

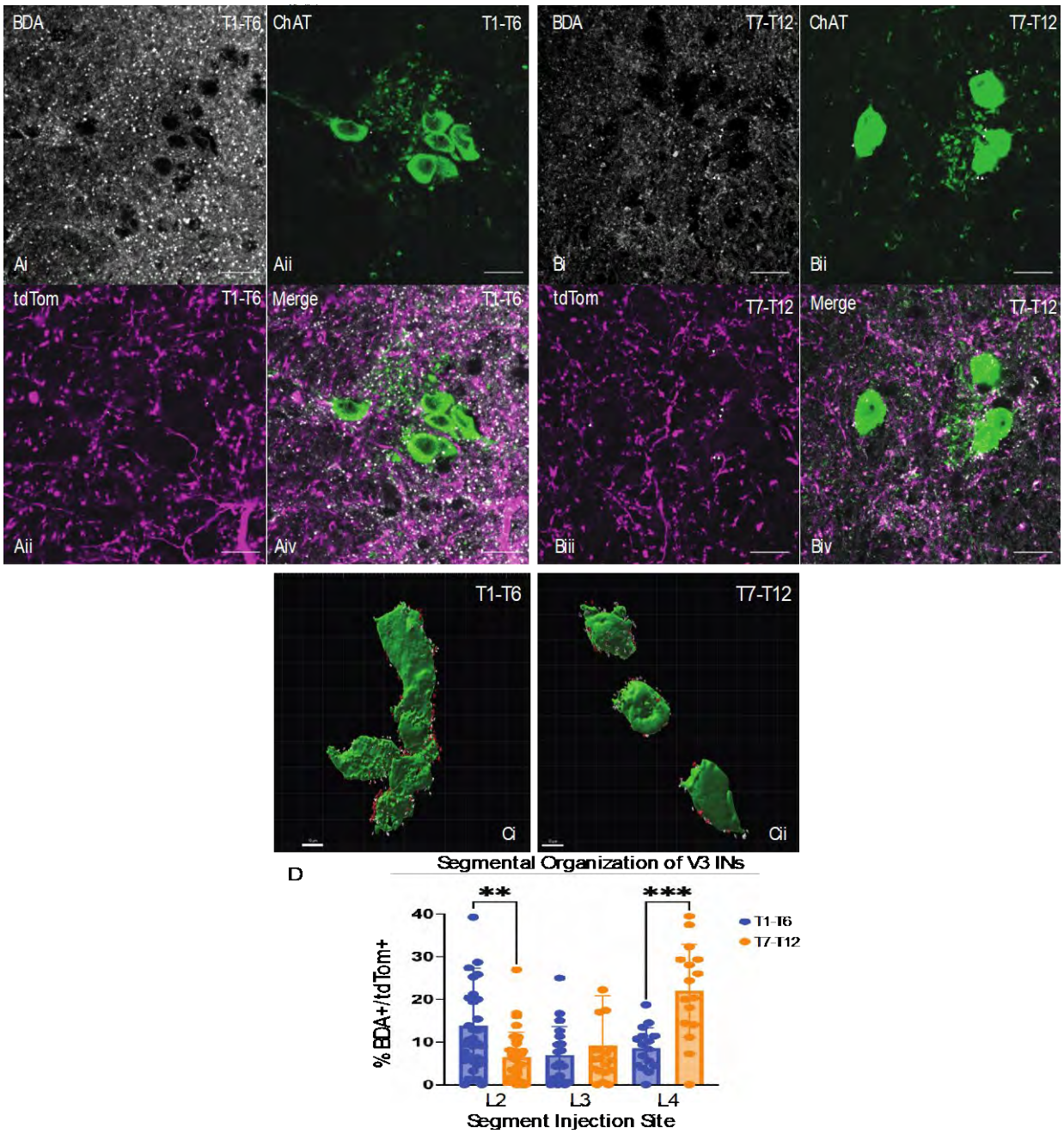


**Figure 10**: **Lumbar V3 INs show distinct thoracic SPN projection profiles, revealed by segmental level of BDA injection site**. Ai-iv & Bi-iv) Co-localized BDA and V3 IN puncta on SPNs in T1-T6 and T7-12 spinal cord indicated by arrow heads. (**Scale** = 20 µm). Ci-ii) 3D reconstructed IMARIS Bitplane image of T1-T6 and T7-12 SPNs, BDA and V3 puncta (**Scale** = 10 µm) D) Percentage of $BDA^{+}/tdTom^{+}$ contacts on SPNs in different mice injected at different

lumbar levels (one way ANOVA and Šidák's multiple comparison tests, **$p<0.0067$, ***$p<0.0004$, n = 4 mice total).

*Distribution of lumbar V3 INs that project to T8 segment*

We then investigated which sub-populations of V3 INs were innervating thoracic SPNs. Our objective was to target our injection to be as close to IML SPNs as possible, avoiding injecting into white matter to prevent uptake by axons of passage. Due to high vasculature near T5-T6 encountered during surgery, CTB was injected more caudally, into the T8 segment of the spinal cord. CTB injections resulted in labelling within all three sub-populations of V3 INs in the lumbar spinal cord. Although numbers of mice used are small, there may be differences in ipsilateral versus contralateral projection patterns for the different populations of V3 INs. Specifically, unilateral injections (**Figure 11** & **12)** show spread of CTB-A488 through the grey matter near the IML. After classifying V3 INs into dorsal, intermediate and ventral sub-populations (**Figure 12B**), we observed similar distributions of labelled cells in ipsilateral and contralateral V3 somas for CTB injections located close to the midline of the spinal cord (**Figure 12A**; 72.7% of dorsal, 48.5% of intermediate and 57.8% of ventral ipsilateral V3 somas versus 69.4% of dorsal, 53.6% of intermediate and 66.3% of ventral contralateral V3 somas, **Figure 13**, **n = 3 mice).** However, in our single mouse with a restricted ipsilateral CTB injection site (**Figure 11**), we observed 73.5% of dorsal, 59.7% of intermediate and 67.6% of ventral ipsilateral V3 somas were $CTB^{+}/tdTom^{+}$ whereas 64.3% of dorsal, 55.1% of intermediate and 67.4% of ventral contralateral V3 somas were $CTB^{+}/tdTom^{+}$ (**n = 1 mouse**) in the lumbar spinal cord (**Figure 13**). This data suggests that neurons within all V3 IN subpopulations project to SPNs and may be responsible for different aspects of regulating sympathetic output or for coordinating locomotor and sympathetic activity. To date, V3 INs have been reported to have contralateral (Zhang et al., 2008; Borowska et al., 2015) and ipsilateral projections (Chopek et

al., 2018). These results further support previous findings and here we show that V3 INs also have projections to ipsilateral spinal regions within the thoracic IML.

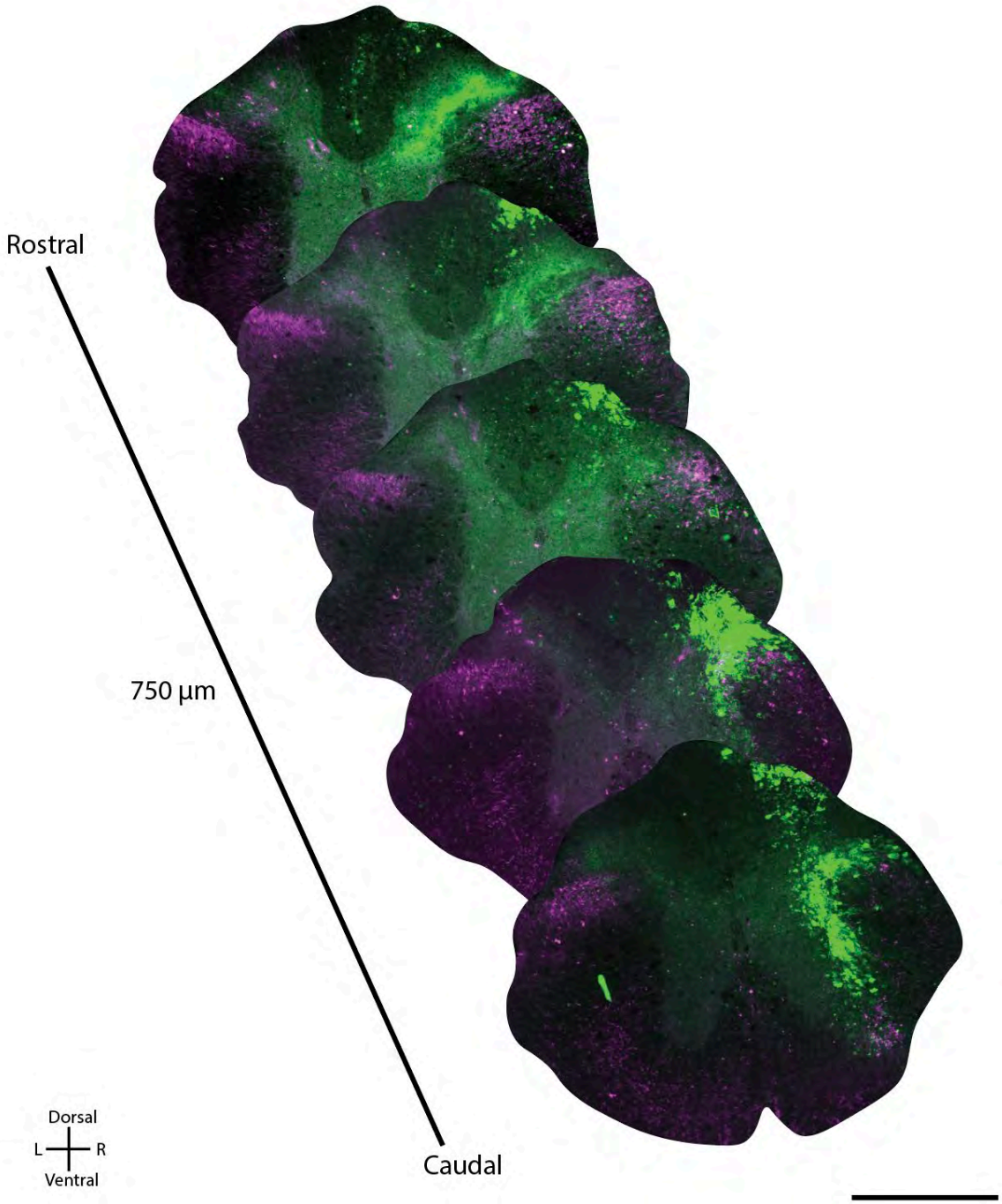


**Figure 11: CTB-A488 unilateral injection site.** Reconstructed unilateral injection site near the T8 spinal segment of CTB-A488 dye (green) in grey matter confined to right side of spinal cord. Axons of passage in the white matter and sparse V3 somas in the grey matter (violet). (**Scale** = 500 µm).

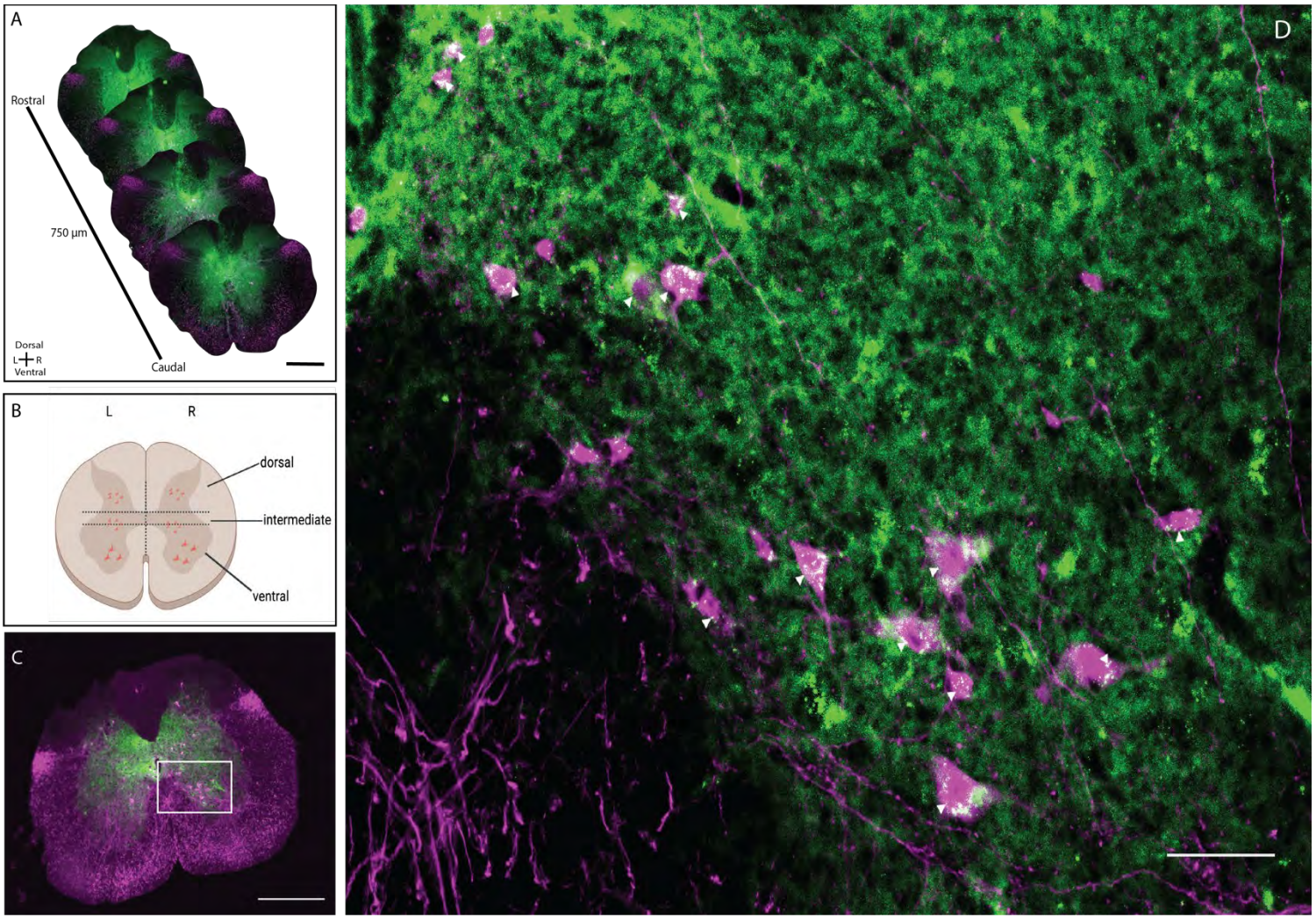


**Figure 12: Dorsal, ventral and intermediate V3 INs project to T8 spinal segment.** A) Reconstructed unilateral injection site of CTB-A488 dye in grey matter of spinal cord (**Scale** = 500 µm) B) Transverse section of lumbar spinal cord showing classification scheme used to separate V3 INs into dorsal, intermediate and ventral subpopulations based on soma location C) L1/L2 spinal cord with double labelled $CTB^+$ (green) and $tdTom^+$ V3 IN somas (violet) (**Scale** = 500 µm) D) Zoomed in portion of panel C showing double labelled $CTB^+$ (green) and $tdTom^+$ V3 IN somas (violet) with arrow heads (**Scale** = 50 µm).

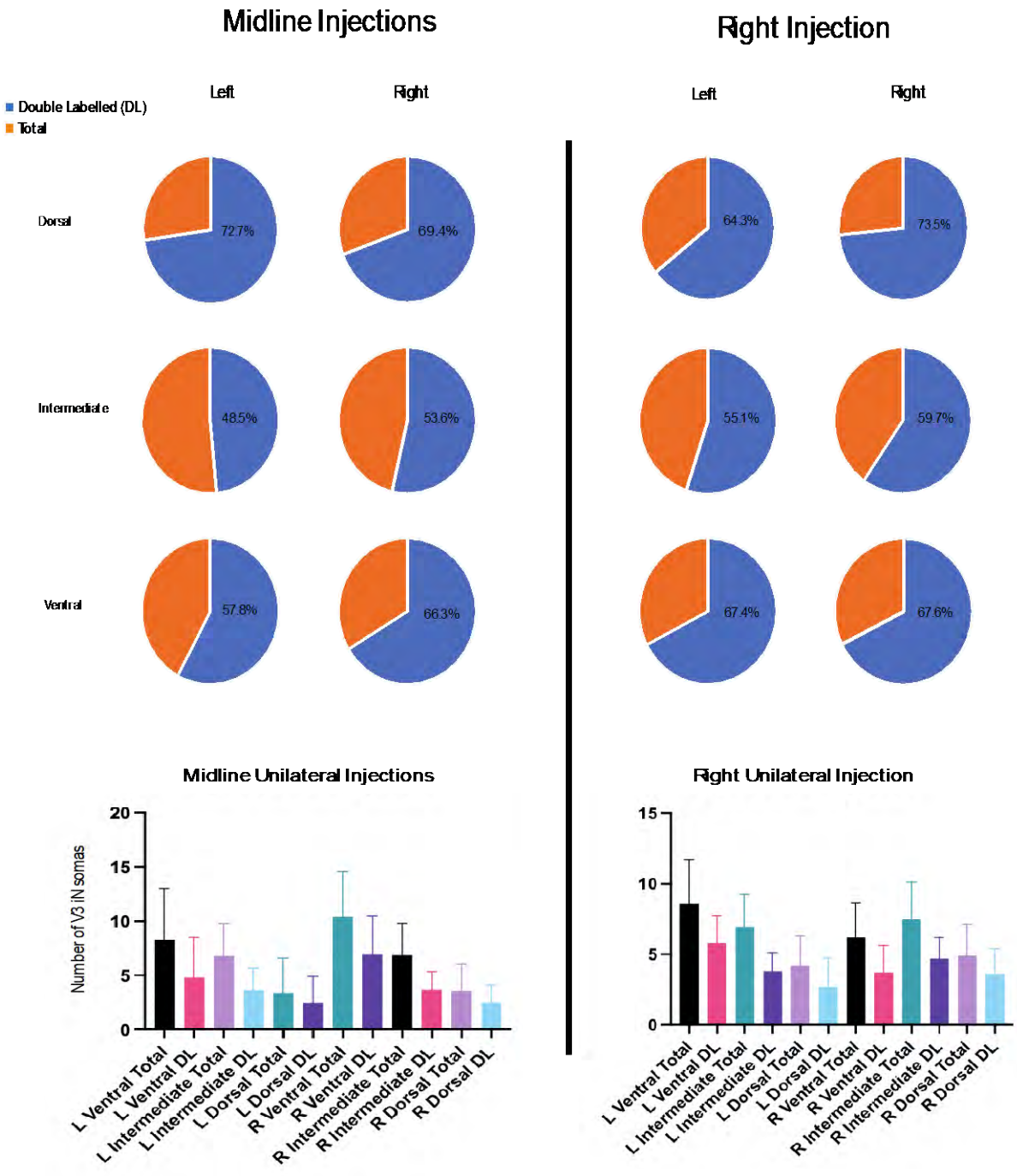


**Figure 13: Between ~50-70% of lumbar V3 INs from dorsal, intermediate and ventral populations project to T8 spinal cord**. Double labelled (DL) $CTB^{+}$/$tdTom^{+}$ somas were observed on ipsi- and contralateral sides of spinal cord in unilateral midline (n = 3 mice) and right (n = 1 mouse) injections.

*Local glutamatergic INs do not project to SPNs in thoracic spinal cord*

Since ~80% of VGlut2 innervation on SPNs remain unaccounted for, we investigated if local propriospinal populations may be providing direct synaptic input to SPNs. Using Chx10 mice which is expressed in V2a INs, we observed that although these neurons have projections within the IML, they are far fewer and do not appear to appose SPNs (**Figure 14**, verified by lack of $VGlut2^{+}/GFP^{+}$ puncta). Thus, populations other than V2a INs should be investigated to determine if any other spinal IN provides direct synaptic input to SPNs.

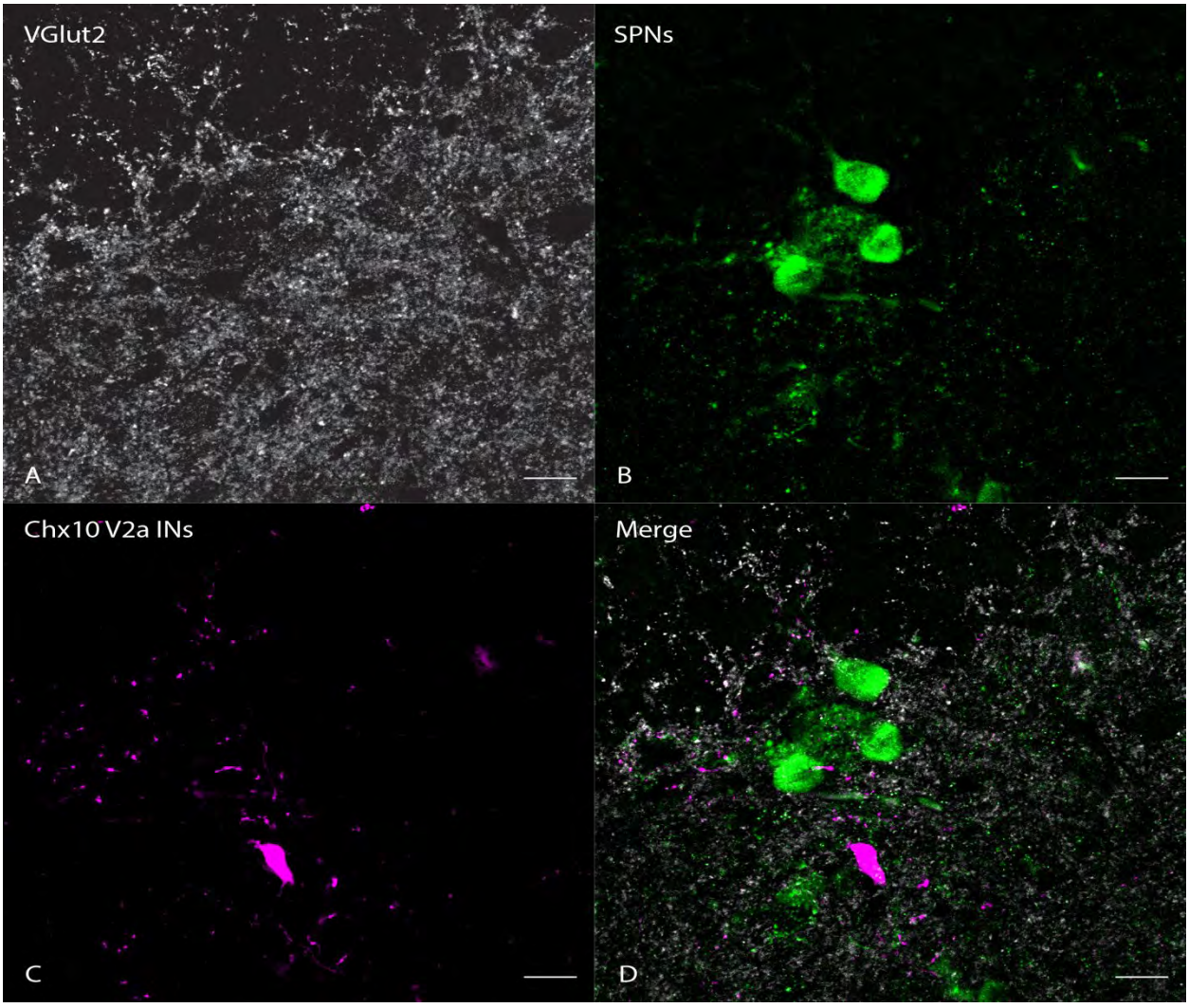


**Figure 14: Local V2a axon terminals show no puncta/projections onto IML SPNs**. A) VGlut2 presynaptic marker B) thoracic SPNs located in IML C) Limited axonal projections of local V2a INs that do not appose SPNs D) Merged image. **Scale** = 20 µm.

# Chapter V: Discussion

## 5.1 Summary of results

This project characterized anatomical connections within thoracic autonomic regions arising from lumbar locomotor-related V3 INs. We showed a significantly greater number of V3 somas in lumbar compared to thoracic regions and a high concentration of V3 IN puncta near the IML. Analysis using IMARIS indicated that that ~20% of all excitatory VGlut2 innervation on SPNs originates from V3 INs with no significant difference in puncta to SA ratios for T1-T6 and T7-T12. However, when grouped by spinal segment, it appears there may be a peak in numbers of V3 IN puncta in mid thoracic segments (T4/T5). All lumbar BDA injections (L2, L3 and L4/5) demonstrated $BDA^+/tdTom^+$ puncta in IML throughout the spinal cord, with different percentages of $BDA^+/tdTom^+$ puncta in T1-T6 and T7-T12 depending on site of injection. Through CTB injections, we also found that between ~50-70% of dorsal, ventral and intermediate V3 INs project within T8 spinal cord. Together, this demonstrates that lumbar V3 INs synapse on autonomic SPNs of the thoracic spinal cord.

## 5.2 V3 soma and puncta distribution in the thoraco-lumbar spinal cord

V3 IN somas were found to be dispersed throughout the thoracic spinal cord but had significantly higher numbers in upper lumbar (mean = 32.85 somas) compared to thoracic regions (mean = 16.6 somas and 14.0 somas for T1-T6 and T7-T12, respectively, * $p < 0.05$, **** $p < 0.0001$). In addition, thoracic V3 IN somas were visually smaller in size compared to dorsal and ventral V3 IN somas of the lumbar spinal cord, consistent with previous findings (Zhang et al., 2008; Borowska et al., 2013, 2015; Blacklaws et al., 2015; Chopek et al., 2018). There are likely higher numbers of V3 INs in the lumbar spinal cord because of their

involvement in the lumbar locomotor CPG, establishing robust and stable locomotor rhythms (Borowska et al. 2013; Goudling, 2009; Zhang et al., 2008).

Early studies showed that the lumbar spinal cord was able to produce activation and coordination of hindlimb muscles during locomotion (Grillner, 1981). Later studies then explored the longitudinal distribution of the mammalian hindlimb locomotor CPG. In isolated rodent spinal cord preparations, it is suggested that the hindlimb locomotor CPG is distributed throughout the lumbar cord, but rostral segments seem to have more "rhythmogenic" capacity than caudal segments (Kiehn, 2006; Cowley & Schmidt, 1997; Kremer & Lev-Tov, 1997). In rostral lumbar segments (L1/L2), L2 BDA injections preferentially projected to T1-T6 segments compared to T7-T12 segments, where T1-T6 sympathetic outflow is known to project to the heart and bronchi (Kandel, 2013; Cowley, 2018). These organs are important in increasing sympathetic activity to increase heart rate, BP, cardiac output and respiratory rate to meet metabolic needs during bouts of exercise and locomotion. Therefore, V3 INs located in L2 may preferentially project to T1-T6 to mediate sympathetic input to these organs and maintain homeostatic needs during times of locomotion or exercise. L3 injections showed no preference in projections to T1-T6 or T7-T12, whereas L4/L5 BDA injections preferentially projected to T7-T12. T7-T12 sympathetic outflow projects to the adrenal medulla, kidneys, liver, stomach, pancreas and small intestine (Cowley, 2018), and it is possible that L4/L5 V3 INs preferentially project to T7-T12 to mediate catecholamine release and digestive responses. However, all of this may simply be related to anatomy and maximum distance each IN can project. Eide & Glover (1996) showed that propriospinal INs project around 4 to 7 segments and the length of individual projections from different spinal levels show a normal distribution in an avian model (Eide &

Glover, 1996). Upper lumbar V3 INs (in L1/L2) may project up to 7 spinal segments which would correspond to projections near T4/T5. Since there are higher numbers of V3 IN somas in L1/L2, the projections of these somas may be responsible for the peak in puncta density observed in T4/T5 spinal segments, with lower lumbar V3 INs (L3-L6) projecting to lower thoracic SPNs based on the maximum distance propriospinal INs are able to project. Ultimately, understanding anatomical connections, segmental organization of V3 INs and their projections on SPNs, may help in understanding how to activate specific SNS tissues and organs to improve sympathetic function in the absence of walking.

There is still controversy, however, over whether the lumbar locomotor CPG is restricted to L1-L2 segments and is “critical” as locomotion can still be evoked when this region is isolated (Kremer & Lev-Tov, 1997; Cowley & Schmidt, 1997). Therefore, although there seems to be segmental preference for L1-L2 V3 INs to project to T1-T6 SPNs and L4/L5 V3 INs to project to T7-T12 SPNs, responsible for cardiac and catecholamine release respectively, it is plausible that V3 IN projections from all lumbar regions may help mediate SPN function throughout the thoracic spinal cord. Thus, preferential V3 IN projections from lumbar segments on thoracic SPNs may be redundant, much like the circuitry responsible for producing and coordinating locomotion (Alstermark et al., 1979; Cowley & Schmidt, 1997; Cazalets, Borde & Clarac, 1995). It may also be possible that V3 INs distributed throughout the thoracic spinal cord may help coordinate locomotor rhythms observed when the lumbar locomotor CPG is ablated (Cowley & Schmidt, 1997). It may also be possible that V3 INs distributed throughout the thoracic spinal cord may help coordinate locomotor rhythms observed when the lumbar locomotor CPG is ablated (Cowley & Schmidt, 1997). It also remains to be seen if V3 INs distributed throughout

the thoracic spinal cord demonstrate similar segmental organization projections like lumbar V3 INs onto thoracic SPNs.

Through quantification of visually distinct densities of V3 IN puncta, a spike in puncta density was observed around the T4/T5 segment. Less V3 puncta innervation was observed in more rostral thoracic segments (~T1-T4), followed by dense puncta innervation near T5 and decreasing of puncta density caudal to T8. At T5, SPNs project not only to the heart and bronchi, but to skin cutaneous vasodilators, sweat glands, arterial smooth muscle, and the greater splanchnic nerve which innervates digestive organs and the adrenal medulla to regulate catecholamine release (Kandel, 2013; Cowley, 2018). The marked spike of V3 IN puncta in the IML near T5 could be due to overlap in sympathetic outflow projections at this specific segment. More V3 INs may innervate SPNs at this segment to mediate and facilitate sympathetic input of the overlapping targets such as the heart, sweat glands, arterial smooth muscle, skin cutaneous vasodilators, bronchi, greater splanchnic nerve and adrenal medulla (Cowley, 2018).

The high density of V3 puncta in the IML may be explained through the dorsal-lateral migratory trajectory of V3 INs, like that of SPNs, mediated by Reelin-related pathways (Blacklaws et al, 2015; Yip et al., 2004; Yip et al., 2009). Reelin does not overlap with V3 INs, suggesting that V3 INs do not produce Reelin. SPNs are found in areas devoid of Reelin such as the ventrolateral spinal cord, suggesting that Reelin could act as a barrier for SPN migration (Yip et al., 2004; Yip et al., 2009). Sim1 is necessary for proper “positional topography” of V3 somas and spatial distribution of V3 IN contralateral axonal trajectories in ventral and dorsal subpopulations (Blacklaws et al., 2015). The expression of Sim1 for proper V3 IN migration and lack of Reelin expression in V3 INs may explain why V3 IN puncta are observed in the IML apposing SPNs

while V3 IN somas are not found in this region, but rather, in their ventral, dorsal and intermediate clusters. Altogether, this data suggests that V3 INs are found throughout the thoracic and lumbar spinal cord but may predominantly project from long ascending V3 INs in the lumbar cord. This may be because of the greater numbers of V3 somas observed in lumbar segments compared to thoracic regions and BDA injections in lumbar spinal regions which show projections to thoracic SPNs. However, we did not investigate projections from thoracic V3 INs onto thoracic SPNs which may also account for V3 IN innervation on SPNs.

### 5.3 Functionality of VGlut2 input on SPNs

ES is thought to activate connections between afferent fibres and sympathetic circuitry following SCI. SPNs are involved increasing sympathetic output and excitation of thoracic SPNs likely involves excitatory INs (Squair et al., 2021). We discovered that VGlut2 expressing lumbar V3 propriospinal locomotor-related spinal neurons have synapses with SPNs located throughout the thoracic spinal cord accounting for ~20% of all excitatory VGlut2 innervation. This VGlut2$^{+}$/tdTom+ apposition may be responsible for improvements seen in cardiac parameters and BP following ES of the lumbar spinal cord (Aslan et al., 2018). When V3 INs or their puncta are optogenetically stimulated, we have been able to record action potentials (APs) from SPNs in the IML (preliminary data, Chopek lab). This suggests that not only do V3 INs have an anatomical connection on SPNs, but they appear to have a functional role in mediating SPN activity and sympathetic outflow.

In addition to loss of descending input, absence of communication between spinal and supraspinal neural circuitry, SCI also alters neurotransmitter receptor expression in neurons

located caudal to the site of injury. Excitatory glutamatergic transmission is believed to be essential for the locomotor CPG in initiating locomotion (Talpalar & Kiehn, 2010). SCI alters the expression of ligand-gated channels which alters the physiology of synapses in spinal interneurons, causing an imbalance of excitatory and inhibitory effects of spinal interneurons which are normally under tight control. Following SCI, synaptic changes cause increased inhibition resulting in impaired signal transduction within spared spinal tissue. It is suggested that activation and modulation of inhibitory interneurons may be important for functional recovery following SCI and therefore, loss of appropriately timed descending input causes lack of movement and function (Zavvarian, Hong & Fehlings, 2020).

Following SCI, Noble and colleagues (2022) suggest that activity-dependent plasticity contributes to autonomic circuitry remodelling and that thoracic VGlut2$^{+}$ INs may coordinate these changes (Noble et al., 2022). Activating VGlut2$^{+}$ INs in naïve mice replicated changes that occur in autonomic networks after SCI and silencing VGlut2$^{+}$ INs prevented aberrant cardiovascular reflexes, suggesting that thoracic VGlut2 INs are important in coordinating these changes (Noble et al., 2022). These findings contradict beneficial clinical observations of improved BP, HR and other autonomic parameters found after ES (e.g., Aslan et al., 2018) which likely involve exciting excitatory INs such as VGlut2 INs. Although chemogenetic silencing of ~20-30% of ipsilateral VGlut2$^{+}$ INs (between the T4 and T8 spinal segments) may be beneficial in targeting thoracic SPNs to prevent aberrant activity after injury, lumbar projecting VGlut2 contacts, such as those from V3 INs, may not undergo the same changes in aberrant autonomic circuitry remodelling and could mediate the improvements seen in ES. We use an intact mice model therefore, it is also possible that following SCI, activating V3 INs may be involved in

aberrant changes observed in the spinal cord. These findings emphasize the importance of understanding the interconnectivity between glutamatergic, locomotor-related and autonomic systems to prevent aberrant circuitry remodelling and to optimize therapeutic strategies for individuals living with SCI.

## 5.4 Projections of different populations of V3 INs

Ventral V3 INs are recruited during swimming and running and are involved in general locomotor activity output. Dorsal V3s are only active during running and are recruited for weight bearing gaits to serve as relay neurons that receive intense sensory inputs to adjust left-right coordination indirectly (Borowska et al., 2013; Laliberte et al., 2019). In our experiments, dorsal ventral and intermediate V3 INs ipsilateral and contralateral to our unilateral injection sites were $CTB^{+}/tdTom^{+}$. This suggests that lumbar V3 INs involved in different aspects of locomotion (general locomotion and recruited for weight bearing gaits) project to T8 and may be responsible for increasing excitatory drive to multiple sympathetic target organs and tissues involved in homeostatic and metabolic support for movement, such as mediating catecholamine release from the adrenal medulla in response to locomotion.

Preliminary finding from the Zhang lab indicated that V3 IN subsets have different molecular, spatial, and axonal projections based on different TFs determined by the embryological date E14.5. The table below (**Table 3**) summarizes different TFs that characterize different V3 IN subtypes in embryonic mice and their respective axonal projections (personal correspondence). It is possible that these embryonic factors could be responsible for projections observed in adult dorsal, ventral and intermediate V3 INs (Blacklaws et al., 2015). Based on our

CTB injections to T8, and that V3 INs are mainly characterized as having contralateral projections, with ipsilateral projections as well (Zhang et al., 2008, Chopek et al., 2018), V3 INs that express Nkr3b3+, Olig3+ and Pouf2b2+ embryonically could be involved in commissural projections to thoracic SPNs from the lumbar spinal cord in adult mice. We also found that ~50-70% of $CTB^{+}$/$tdTom^{+}$ somas were located ipsilateral to our injection site, further supporting previous findings that V3 INs are not solely commissural INs (Chopek et al., 2018). Although ¾ of our preparations had bilateral spread of CTB, we cannot rule out the possibility that ipsilateral $CTB^{+}$/$tdTom^{+}$ somas seen in the lumbar cord could be commissural projections. However, given that in our single mouse with confirmed unilateral spread of CTB, we observed somas located ipsilateral to the injection site, this suggests that V3 INs do provide ipsilateral, in addition to contralateral projections within thoracic spinal segments.

| V3 INs | Transcription Factor | Axon Projections |
|---|---|---|
| | Onecut2+ | Descending ipsilateral |
| | Nkr3b3+ | Ascending commissural |
| | Olig3+ | Primarily commissural descending, some ascending |
| | Pouf2f2+ | Descending ipsilateral, descending commissural, ascending commissural |

**Table 3: Molecular transcription factors of V3 IN subtypes in embryonic mice.**

## 5.5 Investigating other IN subtypes that may appose thoracic SPNs

Since V3 IN innervation accounted for ~20% of total VGlut2 innervation apposing SPNs, we expect that other sources of excitatory input from different brain and spinal neurons to also be involved in SPN innervation. First, we examined whether V2a INs that express Chx10 have synaptic terminals in the IML. V2as are glutamatergic, local and ipsilaterally projecting INs found in the spinal cord that are involved in controlling left-right alternation and densely innervate motoneurons (Goulding, 2009; Dougherty & Kiehn, 2010). Since V2a INs express VGlut2 and innervate motoneurons, they may be another IN candidate that may have VGlut2 contacts on SPNs. Skinner and colleagues (2021) reported that excitatory V2a INs expressing the TF Chx10, in the IML, projected to ventral regions of the spinal cord. Using anterograde tracer, dense innervation of motoneurons from V2a INs in lumbar spinal cord was observed (Skinnider et al., 2021). V2a INs have previously been demonstrated to project to the IML, but this was only examined in the lumbar cord. However, when examined in the thoracic spinal cord, we did not see any contacts within the IML. V2 INs likely produce Reelin and overlap with Reelin-occupying areas in SPN migration whereas SPNs occupy regions devoid of Reelin (Yip et al., 2004, 2009). This is likely why we do not observe V2a IN projections onto SPNs in the thoracic spinal cord.

DBX expressing V0 INs are also known to be glutamatergic INs and our preliminary unpublished findings suggest that there are no $VGlut2^{+}/Dbx^{+}$ puncta apposing SPNs in thoracic spinal cord. Therefore, it is possible that there are other presumably glutamatergic cell types providing excitatory synaptic input to SPNs (Guyenet et al., 2013; Ueno et al., 2016; Noble et al., 2022), such as C1 neurons found in the IML (Guyenet et al., 2013). It is also possible that other

cell types that are not interneuron in origin, appose and provide input to SPNs. Other sources that express VGlut2 include the medial reticular formation (medRF) locomotor centre, cardio-respiratory centres and vestibulo-sympathetic pathways. These sources all have descending, excitatory, glutamatergic neurons (Noga et al., 2003; Bretzner & Brownstone, 2013; Spyer & Gourine, 2009; Holstein, Friedrich & Martinelli, 2016) that may appose SPNs to mediate sympathetic outflow. This may make V3 INs the only spinal IN population mediating connections on SPNs, particularly in the ascending direction. Altogether, these findings provide strong anatomical evidence that V3 INs provide direct glutamatergic contacts on SPNs. The source of other glutamatergic input remains to be determined, but it is unlikely to include V2a INs or V0 INs.

## 5.6 Limitations

One limitation to our findings regarding CTB-A488 injections was that injections were not restricted to one side of the spinal cord. Thus, although we performed unilateral injections, 3 of our 4 injected mice showed dye spread bilaterally through grey matter of the spinal cord. As such, we were only able to make observations regarding side-specific projections from one mouse. It is possible that in our injections, CTB may have been taken up by axons of passage, resulting in higher numbers of V3 somas being $CTB^{+}/tdTom^{+}$. Therefore, certain V3 IN (dorsal, ventral and intermediate ipsilateral and contralateral) populations may not play as much of a role in projecting to the T8 spinal segment. To overcome this limitation, two tracer dyes (Fluoro-Gold and CTB) could be injected unilaterally into either the white matter or grey matter of the spinal cord to distinguish between axons of passage and true projections of V3 somas.

Another limitation relates to our calculation of SA to puncta ratios. We hypothesized that there would be a significant difference in the SA to puncta ratios to further support the notion of segmental organization of V3 IN projections from the lumbar spinal cord, however there were no significant differences in T1-T6 compared to T7-T12 spinal segments for $VGlut2^{+}/tdTom^{+}$ and $BDA^{+}/tdTom^{+}$. This discrepancy may be completely methodological since our segmentation may have been too course to observe any somatotopic organization of the organization of the projection patterns from lumbar V3 INs. This is supported by our observations of peaks in puncta observed at the T4/T5 spinal levels (**Figure 6**). Thus, in future experiments spinal segments could be further subdivided in order to investigate differences of VGlut2 on all spinal segments. There is also variability between sizes of individual SPNs and the number of puncta to these specific SPNs. This variability could affect the ratio number, thus, to overcome this limitation, SPNs that fall between a certain SA range (such as 500-700 $\mu m^2$) could be analyzed to reduce variability and see stronger trends for segmental preference in BDA injected mice.

# Chapter VI: Conclusion

## 6.1 Key Findings

This is the first demonstration of locomotor-related spinal neurons have projections onto autonomic cells located throughout the thoracic spinal cord. Quantitative analysis done in IMARIS revealed that ~20% of VGlut2 projections apposing SPNs are V3 in origin with no significant differences between T1-T6 and T7-T12 segments. All lumbar BDA injections (L2, L3 and L4/5) demonstrated $BDA^{+}/tdTom^{+}$ puncta in IML throughout the spinal cord, with segmental organization of $BDA^{+}/tdTom^{+}$ puncta in T1-T6 and T7-T12 depending on the BDA injection site. CTB injections revealed that dorsal, ventral and intermediate V3 INs are project to the T8 segment. Characterization of projections from lumbar propriospinal INs within the spinal cord revealed that V3 INs had anatomical connections onto thoracic autonomic SPNs. V3 INs and their anatomical projections may be responsible for cardiac and other autonomic improvements seen following ES, and these findings may provide greater insight into rehabilitative strategies to regain both locomotor and sympathetic function following injury.

## 6.2 Future Directions

Ultimately, these results demonstrate a further need to understand the spinal cord and its ability to integrate locomotor and sympathetic activity. Ongoing work in our lab is investigating functional roles of V3 INs in mediating SPN activity and sympathetic outflow. Using an optogenetic mouse line, we are investigating if stimulation of V3 somas and or their terminals can elicit APs in thoracic SPNs. This work will likely reveal novel ways in which SPNs respond to V3 IN activity.

It is likely that lumbar V3 IN populations provide the only spinal source of input onto SPNs given that V3 INs are found in the thoracic cord and may provide local projections on thoracic SPNs. Further tracer injection studies into thoracic and or cervical spinal segments could reveal the percentage of descending and local thoracic V3 INs that provide input on SPNs compared to lumbar V3 INs. Identification and characterization of other VGlut2$^{+}$ sources on SPNs may also provide more insight on the ascending/descending connections that appose SPNs and how they may be affecting their function.

Translationally, this knowledge may provide greater insight into optimization of therapeutic strategies for individuals living with SCI. These findings may help in ES specificity for segmental targeting of sympathetic output to specific organs or targets of interest depending on injury level. For example, if the goal is to improve cardiovascular parameters, ES may be placed over L1/L2 whereas ES placed over L3/L4/L5 may be used to target catecholamine release. Novel anatomical connections found in this study between lumbar V3 propriospinal INs

and autonomic SPNs provide insight into understanding the integration between locomotor and sympathetic function.

## References


- Anderson, K.D. (2004) Targeting recovery: priorities of the spinal cord-injured population. J Neurotrauma, **21**, 1371-1383.
- Aslan, S.C., Legg Ditterline, B.E., Park, M.C., Angeli, C.A., Rejc, E., Chen, Y., Ovechkin, A.V., Krassioukov, A. & Harkema, S.J. (2018) Epidural Spinal Cord Stimulation of Lumbosacral Networks Modulates Arterial Blood Pressure in Individuals With Spinal Cord Injury-Induced Cardiovascular Deficits. *Front Physiol*, **9**, 565-565.
- Baldauf, K.J., Royal, J.M., Hamorsky, K.T. & Matoba, N. (2015) Cholera Toxin B: One Subunit with Many Pharmaceutical Applications. *Toxins*, **7**, 974-996.
- Blacklaws, J., Deska-Gauthier, D., Jones, C.T., Petracca, Y.L., Liu, M., Zhang, H., Fawcett, J.P., Glover, J.C., Lanuza, G.M. & Zhang, Y. (2015) Sim1 is required for the migration and axonal projections of V3 interneurons in the developing mouse spinal cord. Dev Neurobiol, **75**, 1003-1017.
- Borowska, J., Jones, C.T., Deska-Gauthier, D. & Zhang, Y. (2015) V3 interneuron subpopulations in the mouse spinal cord undergo distinctive postnatal maturation processes. *Neuroscience*, **295**, 221-228.
- Borowska, J., Jones, C.T., Zhang, H., Blacklaws, J., Goulding, M. & Zhang, Y. (2013) Functional subpopulations of V3 interneurons in the mature mouse spinal cord. *J Neurosci*, **33**, 18553-18565.
- Bretzner, F. & Brownstone, R.M. (2013) Lhx3-Chx10 reticulospinal neurons in locomotor circuits. *The Journal of neuroscience : the official journal of the Society for Neuroscience*, **33**, 14681-14692.
- Brown, T.G. (1911) The intrinsic factors in the act of progression in the mammal. *Proceedings of the Royal Society of London. Series B, Containing Papers of a Biological Character*, **84**, 308–319.
- Brown, T.G. (1914) On the nature of the fundamental activity of the nervous centres; together with an analysis of the conditioning of rhythmic activity in progression, and a theory of the evolution of function in the nervous system. *J Physiol*, **48**, 18-46.
- Brown, W. & Deiters, A. (2019) Chapter Thirteen - Light-activation of Cre recombinase in zebrafish embryos through genetic code expansion. In Deiters, A. (ed) Methods in Enzymology. Academic Press, pp. 265-281.
- Brownstone, R.M. & Bui, T.V. (2010) Spinal interneurons providing input to the final common path during locomotion. *Prog Brain Res*, **187**, 81-95.
- Cherniak, M., Etlin, A., Strauss, I., Anglister, L. & Lev-Tov, A. (2014) The sacral networks and neural pathways used to elicit lumbar motor rhythm in the rodent spinal cord. Front Neural Circuits, **8**, 143.
- Chopek, J.W., Nascimento, F., Beato, M., Brownstone, R.M. & Zhang, Y. (2018) Sub-populations of Spinal V3 Interneurons Form Focal Modules of Layered Pre-motor Microcircuits. Cell Rep, **25**, 146-156.e143.
- Chopek, J.W., Zhang, Y. & Brownstone, R.M. (2021) Intrinsic brainstem circuits comprised of Chx10-expressing neurons contribute to reticulospinal output in mice. *J Neurophysiol*.
- Chopra, A.S., Miyatani, M. & Craven, B.C. (2018) Cardiovascular disease risk in individuals with chronic spinal cord injury: Prevalence of untreated risk factors and poor adherence to treatment guidelines. *J Spinal Cord Med*, **41**, 2-9.

- Conte, W.L., Kamishina, H., & Reep, R.L. (2009) Multiple neuroanatomical tract-tracing using fluorescent Alexa Fluor conjugates of cholera toxin subunit B in rats. *Nature Protocols*, **4**, 1157–1166.
- Cowley, K.C. (2018) A new conceptual framework for the integrated neural control of locomotor and sympathetic function: implications for exercise after spinal cord injury. Appl Physiol Nutr Metab, **43**, 1140-1150.
- Cowley, K.C. & Schmidt, B.J. (1997) Regional distribution of the locomotor pattern-generating network in the neonatal rat spinal cord. *J Neurophysiol*, **77**, 247-259.
- Cowley, K.C., Zaporozhets, E. & Schmidt, B.J. (2010) Propriospinal transmission of the locomotor command signal in the neonatal rat. Ann N Y Acad Sci, **1198**, 42-53.
- Dederen, P.J.W.C., Gribnau, A.A.M., & Curfs, M.H.J.M. (1994) Retrograde neuronal tracing with cholera toxin B subunit: comparison of three different visualization methods. *The Histochemical Journal*, **26**, 856–862.
- Deska-Gauthier, D., Borowksa, J. & Zhang, Y. (2021) Excitatory spinal V3 interneuron subpopulations diversify across hierarchical temporal and spatial developmental pathways. Poster session presented at: Society for Neuroscience 2021; 2021 Nov 8-11; Chicago, IL.
- Deska-Gauthier, D., Borowska-Fielding, J., Jones, C.T. & Zhang, Y. (2020) The Temporal Neurogenesis Patterning of Spinal p3-V3 Interneurons into Divergent Subpopulation Assemblies. J Neurosci, **40**, 1440-1452.
- Devivo, M.J. (2012) Epidemiology of traumatic spinal cord injury: trends and future implications. Spinal Cord, **50**, 365-372.
- Dougherty, K.J. & Kiehn, O. (2010) Firing and Cellular Properties of V2a Interneurons in the Rodent Spinal Cord. *The Journal of Neuroscience*, **30**, 24–37.
- Douglas, J.R., Noga, B.R., Dai, X. & Jordan, L.M. (1993) The effects of intrathecal administration of excitatory amino acid agonists and antagonists on the initiation of locomotion in the adult cat. *J Neurosci*, **13**, 990-1000.
- Duan, B., Cheng, L., Bourane, S., Britz, O., Padilla, C., Garcia-Campmany, L., Krashes, M., Knowlton, W., Velasquez, T., Ren, X., Sarah, Bradford, Wang, Y., Goulding, M., & Ma, Q. (2014) Identification of Spinal Circuits Transmitting and Gating Mechanical Pain. *Cell*, **159**, 1417–1432.
- Eckert, M.J. & Martin, M.J. (2017) Trauma: Spinal Cord Injury. Surg Clin North Am, **97**, 1031-1045.
- Eide, A.L. & Glover, J.C. (1996) Development of an Identified Spinal Commissural Interneuron Population in an Amniote: Neurons of the Avian Hofmann Nuclei. *The Journal of Neuroscience*, **16**, 5749-5761.
- Eldahan, K.C. & Rabchevsky, A.G. (2018) Autonomic dysreflexia after spinal cord injury: Systemic pathophysiology and methods of management. *Autonomic Neuroscience*, **209**, 59-70.
- English, A.W., Tigges, J. & Lennard, P.R. (1985) Anatomical organization of long ascending propriospinal neurons in the cat spinal cord. *J Comp Neurol*, **240**, 349-358.
- Flett, S., Garcia, J. & Cowley, K.C. (2022) Spinal electrical stimulation to improve sympathetic autonomic functions needed for movement and exercise after spinal cord injury: a scoping clinical review. *J Neurophysiol*.

- Gerasimenko, Y., Roy, R.R. & Edgerton, V.R. (2008) Epidural stimulation: Comparison of the spinal circuits that generate and control locomotion in rats, cats and humans. Experimental Neurology, **209**, 417-425.
- Gómara-Toldrà, N., Sliwinski, M. & Dijkers, M.P. (2014) Physical therapy after spinal cord injury: a systematic review of treatments focused on participation. J Spinal Cord Med, **37**, 371-379.
- Goulding, M. (2009) Circuits controlling vertebrate locomotion: moving in a new direction. Nat Rev Neurosci, **10**, 507-518.
- Grätsch, S., Büschges, A. & Dubuc, R. (2019) Descending control of locomotor circuits. Current Opinion in Physiology, **8**, 94-98.
- Grillner, S. (1981) Control of Locomotion in Bipeds, Tetrapods, and Fish. *Comprehensive Physiology*, 1179-1236.
- Grillner, S. & Kozlov, A. (2021) The CPGs for Limbed Locomotion–Facts and Fiction. *International Journal of Molecular Sciences*, **22**, 5882.
- Guertin, P.A. (2013) Central pattern generator for locomotion: anatomical, physiological, and pathophysiological considerations. Front Neurol, **3**, 183-183.
- Harkema, S., Gerasimenko, Y., Hodes, J., Burdick, J., Angeli, C., Chen, Y., Ferreira, C., Willhite, A., Rejc, E., Grossman, R.G. & Edgerton, V.R. (2011) Effect of epidural stimulation of the lumbosacral spinal cord on voluntary movement, standing, and assisted stepping after motor complete paraplegia: a case study. *The Lancet*, **377**, 1938-1947.
- Harrison, M., O'Brien, A., Adams, L., Cowin, G., Ruitenberg, M.J., Sengul, G. & Watson, C. (2013) Vertebral landmarks for the identification of spinal cord segments in the mouse. NeuroImage, **68**, 22-29.
- Holstein, G.R., Friedrich, V.L., Jr. & Martinelli, G.P. (2016) Glutamate and GABA in Vestibulo-Sympathetic Pathway Neurons. *Frontiers in neuroanatomy*, **10**, 7-7.
- Hou, S. & Rabchevsky, A.G. (2014) Autonomic consequences of spinal cord injury. Compr Physiol, **4**, 1419-1453.
- Jain, N.B., Ayers, G.D., Peterson, E.N., Harris, M.B., Morse, L., O'Connor, K.C. & Garshick, E. (2015) Traumatic Spinal Cord Injury in the United States, 1993-2012. JAMA, **313**, 2236-2243.
- Jankowska, E. (1992) Interneuronal relay in spinal pathways from proprioceptors. *Prog Neurobiol*, **38**, 335-378.
- Jankowska, E. (2008) Spinal interneuronal networks in the cat: elementary components. Brain Res Rev, **57**, 46-55.
- Jordan, L.M. (1998) Initiation of locomotion in mammals. *Ann N Y Acad Sci*, **860**, 83-93.
- Jung, H. & Dasen, J.S. (2015) Evolution of Patterning Systems and Circuit Elements for Locomotion, *Dev Cell*, **32**, 408-422.
- Juvin, L., Simmers, J. & Morin, D. (2005) Propriospinal circuitry underlying interlimb coordination in mammalian quadrupedal locomotion. *J Neurosci*, **25**, 6025-6035.
- Kandel, E.R. (2013) *Principles of neural science*. McGraw-Hill Medical, New York.
- Kawai, R., Markman, T., Poddar, R., Ko, R., Fantana, A.L., Dhawale, A.K., Kampff, A.R. & Ölveczky, B.P. (2015) Motor cortex is required for learning but not for executing a motor skill. *Neuron*, **86**, 800-812.
- Kiehn, O. (2006) LOCOMOTOR CIRCUITS IN THE MAMMALIAN SPINAL CORD. *Annual Review of Neuroscience*, **29**, 279–306.

- Kiehn, O. & Kjaerulff, O. (1998) Distribution of central pattern generators for rhythmic motor outputs in the spinal cord of limbed vertebrates. *Ann N Y Acad Sci*, **860**, 110-129.
- Kremer, E. & Lev-Tov, A. (1997) Localization of the spinal network associated with generation of hindlimb locomotion in the neonatal rat and organization of its transverse coupling system. *J Neurophysiol*, **77**, 1155-1170.
- Lai, B.-Q., Qiu, X.-C., Zhang, K., Zhang, R.-Y., Jin, H., Li, G., Shen, H.-Y., Wu, J.-L., Ling, E.-A., & Zeng, Y.-S. (2015) Cholera Toxin B Subunit Shows Transneuronal Tracing after Injection in an Injured Sciatic Nerve. *PLOS ONE*, **10**, e0144030.
- Laliberte, A.M., Goltash, S., Lalonde, N.R. & Bui, T.V. (2019) Propriospinal Neurons: Essential Elements of Locomotor Control in the Intact and Possibly the Injured Spinal Cord. Front Cell Neurosci, **13**, 512.
- Lazarov, N.E. (2013) Neuroanatomical tract-tracing using biotinylated dextran amine. Methods Mol Biol, **1018**, 323-334.
- Le Gal, J.P., Juvin, L., Cardoit, L. & Morin, D. (2016) Bimodal Respiratory-Locomotor Neurons in the Neonatal Rat Spinal Cord. *J Neurosci*, **36**, 926-937.
- Legg Ditterline, B., Harkema, S.J., Willhite, A., Stills, S., Ugiliweneza, B. & Rejc, E. (2020) Epidural stimulation for cardiovascular function increases lower limb lean mass in individuals with chronic motor complete spinal cord injury. *Exp Physiol*, **105**, 1684-1691.
- Leong, T.Y. & Leong, A.S. (2007) How does antigen retrieval work? Adv Anat Pathol, **14**, 129-131.
- Llewellyn-Smith, I.J. (2009) Anatomy of synaptic circuits controlling the activity of sympathetic preganglionic neurons. *J Chem Neuroanat*, **38**, 231-239.
- Llewellyn-Smith, I.J., Weaver, L.C. & Keast, J.R. (2006) Effects of spinal cord injury on synaptic inputs to sympathetic preganglionic neurons. In Weaver, L.C., Polosa, C. (eds) *Progress in Brain Research*. Elsevier, pp. 11-26.
- Loewy, P.A.N.A.D., Loewy, A.D., Spyer, K.M. & Press, O.U. (1990) *Central Regulation of Autonomic Functions*. Oxford University Press.
- Marques, S.A., Garcez, V.F., Del Bel, E.A. & Martinez, A.M. (2009) A simple, inexpensive and easily reproducible model of spinal cord injury in mice: morphological and functional assessment. *J Neurosci Methods*, **177**, 183-193.
- Mauri, M., Elli, T., Caviglia, G., Uboldi, G., & Azzi, M. (2017) RAWGraphs. In .
- McCammon, J.R. & Ethans, K. (2011) Spinal cord injury in Manitoba: a provincial epidemiological study. J Spinal Cord Med, **34**, 6-10.
- McCrea, D.A. & Rybak, I.A. (2008) Organization of mammalian locomotor rhythm and pattern generation. Brain Res Rev, **57**, 134-146.
- McKay, W.B., Ovechkin, A.V., Vitaz, T.W., Terson de Paleville, D.G. & Harkema, S.J. (2011a) Neurophysiological characterization of motor recovery in acute spinal cord injury. Spinal Cord, **49**, 421-429.
- McKay, W.B., Ovechkin, A.V., Vitaz, T.W., Terson de Paleville, D.G. & Harkema, S.J. (2011b) Long-lasting involuntary motor activity after spinal cord injury. Spinal Cord, **49**, 87-93.
- Minassian, K., Persy, I., Rattay, F., Pinter, M.M., Kern, H. & Dimitrijevic, M.R. (2007) Human lumbar cord circuitries can be activated by extrinsic tonic input to generate locomotor-like activity. Hum Mov Sci, **26**, 275-295.

- Moechars, D., Weston, M.C., Leo, S., Callaerts-Vegh, Z., Goris, I., Daneels, G., Buist, A., Cik, M., van der Spek, P., Kass, S., Meert, T., D'Hooge, R., Rosenmund, C. & Hampson, R.M. (2006) Vesicular glutamate transporter VGLUT2 expression levels control quantal size and neuropathic pain. *The Journal of neuroscience: the official journal of the Society for Neuroscience*, **26**, 12055-12066.
- Noble, B.T., Brennan, F.H., Wang, Y., Guan, Z., Mo, X., Schwab, J.M., & Popovich, P.G. (2022) Thoracic VGluT2+ Spinal Interneurons Regulate Structural and Functional Plasticity of Sympathetic Networks after High-Level Spinal Cord Injury. *The Journal of Neuroscience*, **42**, 3659–3675.
- Noga, B.R., Kettler, J. & Jordan, L.M. (1988) Locomotion produced in mesencephalic cats by injections of putative transmitter substances and antagonists into the medial reticular formation and the pontomedullary locomotor strip. *J Neurosci*, **8**, 2074-2086.
- Noga, B.R., Kriellaars, D.J., Brownstone, R.M. & Jordan, L.M. (2003) Mechanism for activation of locomotor centers in the spinal cord by stimulation of the mesencephalic locomotor region. *J Neurophysiol*, **90**, 1464-1478.
- Noonan, V.K., Fingas, M., Farry, A., Baxter, D., Singh, A., Fehlings, M.G. & Dvorak, M.F. (2012) Incidence and Prevalence of Spinal Cord Injury in Canada: A National Perspective. *Neuroepidemiology*, **38**, 219-226.
- Rabchevsky, A.G. (2006) Segmental organization of spinal reflexes mediating autonomic dysreflexia after spinal cord injury. Prog Brain Res, **152**, 265-274.
- Reiner, A., Veenman, C.L., Medina, L., Jiao, Y., Del Mar, N. & Honig, M.G. (2000) Pathway tracing using biotinylated dextran amines. *Journal of Neuroscience Methods*, **103**, 23-37.
- Rybak, I.A., Stecina, K., Shevtsova, N.A. & McCrea, D.A. (2006) Modelling spinal circuitry involved in locomotor pattern generation: insights from the effects of afferent stimulation. J Physiol, **577**, 641-658.
- Saleeba, C., Dempsey, B., Le, S., Goodchild, A. & McMullan, S. (2019) A Student's Guide to Neural Circuit Tracing. *Front Neurosci*, **13**, 897.
- Sato, A. (1997) Neural mechanisms of autonomic responses elicited by somatic sensory stimulation. *Neuroscience and Behavioral Physiology*, **27**, 610-621.
- Savic, G., DeVivo, M.J., Frankel, H.L., Jamous, M.A., Soni, B.M. & Charlifue, S. (2017) Causes of death after traumatic spinal cord injury-a 70-year British study. *Spinal Cord*, **55**, 891-897.
- Schober, A. & Unsicker, K. (2001) Growth and neurotrophic factors regulating development and maintenance of sympathetic preganglionic neurons *International Review of Cytology*. Academic Press, pp. 37-76.
- Sharif-Alhoseini, M., Khormali, M., Rezaei, M., Safdarian, M., Hajighadery, A., Khalatbari, M.M., Safdarian, M., Meknatkhah, S., Rezvan, M., Chalangari, M., Derakhshan, P. & Rahimi-Movaghar, V. (2017) Animal models of spinal cord injury: a systematic review. *Spinal Cord*, **55**, 714-721.
- Shefchyk, S.J., Jell, R.M. & Jordan, L.M. (1984) Reversible cooling of the brainstem reveals areas required for mesencephalic locomotor region evoked treadmill locomotion. *Exp Brain Res*, **56**, 257-262.
- Shepard, C.T., Pocratsky, A.M., Brown, B.L., Van Rijswijck, M.A., Zalla, R.M., Burke, D.A., Morehouse, J.R., Riegler, A.S., Whittemore, S.R., & Magnuson, D.S. (2021) Silencing long ascending propriospinal neurons after spinal cord injury improves hindlimb stepping in the adult rat. *eLife*, **10**.

- Sherrington, C.S. (1910) Flexion-reflex of the limb, crossed extension-reflex, and reflex stepping and standing. *The Journal of Physiology*, **40**, 28–121.
- Shik, M.L., Severin, F.V. & Orlovskiĭ, G.N. (1966) [Control of walking and running by means of electric stimulation of the midbrain]. *Biofizika*, **11**, 659-666.
- Skinnider, M.A., Squair, J.W., Kathe, C., Anderson, M.A., Gautier, M., Matson, K.J.E., Milano, M., Hutson, T.H., Barraud, Q., Phillips, A.A., Foster, L.J., La Manno, G., Levine, A.J., & Courtine, G. (2021) Cell type prioritization in single-cell data. *Nature Biotechnology*, **39**, 30–34.
- Smith, C.C., Paton, J.F.R., Chakrabarty, S., & Ichiyama, R.M. (2017) Descending Systems Direct Development of Key Spinal Motor Circuits. *The Journal of Neuroscience*, **37**, 6372–6387.
- Spyer, K.M. & Gourine, A.V. (2009) Chemosensory pathways in the brainstem controlling cardiorespiratory activity. *Philos Trans R Soc Lond B Biol Sci*, **364**, 2603-2610.
- Squair, J.W., Gautier, M., Mahe, L., Soriano, J.E., Rowald, A., Bichat, A., Cho, N., Anderson, M.A., James, N.D., Gandar, J., Incognito, A.V., Schiavone, G., Sarafis, Z.K., Laskaratos, A., Bartholdi, K., Demesmaeker, R., Komi, S., Moerman, C., Vaseghi, B., Scott, B., Rosentreter, R., Kathe, C., Ravier, J., Mccracken, L., Kang, X., Vachicouras, N., Fallegger, F., Jelescu, I., Cheng, Y., Li, Q., Buschman, R., Buse, N., Denison, T., Dukelow, S., Charbonneau, R., Rigby, I., Boyd, S.K., Millar, P.J., Moraud, E.M., Capogrosso, M., Wagner, F.B., Barraud, Q., Bezard, E., Lacour, S.P., Bloch, J., Courtine, G., & Phillips, A.A. (2021) Neuroprosthetic baroreflex controls haemodynamics after spinal cord injury. *Nature*, **590**, 308–314.
- Steeves, J.D. & Jordan, L.M. (1980) Localization of a descending pathway in the spinal cord which is necessary for controlled treadmill locomotion. *Neurosci Lett*, **20**, 283-288.
- Steeves, J.D. & Jordan, L.M. (1984) Autoradiographic demonstration of the projections from the mesencephalic locomotor region. *Brain Research*, **307**, 263-276.
- Stepien, A.E. & Arber, S. (2008) Probing the locomotor conundrum: descending the 'V' interneuron ladder. *Neuron*, **60**, 1-4.
- Steuer, I. & Guertin, P.A. (2019) Central pattern generators in the brainstem and spinal cord: an overview of basic principles, similarities and differences. Rev Neurosci, **30**, 107-164.
- Stoeckel, K., Schwab, M. & Thoenen, H. (1977) Role of gangliosides in the uptake and retrograde axonal transport of cholera and tetanus toxin as compared to nerve growth factor and wheat germ agglutinin. *Brain Research*, **132**, 273-285.
- Svoboda, K. & Li, N. (2018) Neural mechanisms of movement planning: motor cortex and beyond. *Curr Opin Neurobiol*, **49**, 33-41.
- Sylos-Labini, F., Zago, M., Guertin, P.A., Lacquaniti, F. & Ivanenko, Y.P. (2017) Muscle Coordination and Locomotion in Humans. *Curr Pharm Des*, **23**, 1821-1833.
- Talpalar, A.E. & Kiehn, O. (2010) Glutamatergic mechanisms for speed control and network operation in the rodent locomotor CpG. *Front Neural Circuits*, **4**.
- Tashima, R., Koga, K., Yoshikawa, Y., Sekine, M., Watanabe, M., Tozaki-Saitoh, H., Furue, H., Yasaka, T. & Tsuda, M. (2021) A subset of spinal dorsal horn interneurons crucial for gating touch-evoked pain-like behavior. *Proceedings of the National Academy of Sciences*, **118**, e2021220118.

- Ueno, M., Ueno-Nakamura, Y., Niehaus, J., Popovich, P.G. & Yoshida, Y. (2016) Silencing spinal interneurons inhibits immune suppressive autonomic reflexes caused by spinal cord injury. *Nature Neuroscience*, **19**, 784-787.
- Wagner, F.B., Mignardot, J.-B., Le Goff-Mignardot, C.G., Demesmaeker, R., Komi, S., Capogrosso, M., Rowald, A., Seáñez, I., Caban, M., Pirondini, E., Vat, M., Mccracken, L.A., Heimgartner, R., Fodor, I., Watrin, A., Seguin, P., Paoles, E., Van Den Keybus, K., Eberle, G., Schurch, B., Pralong, E., Becce, F., Prior, J., Buse, N., Buschman, R., Neufeld, E., Kuster, N., Carda, S., Von Zitzewitz, J., Delattre, V., Denison, T., Lambert, H., Minassian, K., Bloch, J., & Courtine, G. (2018) Targeted neurotechnology restores walking in humans with spinal cord injury. *Nature*, **563**, 65–71.
- Weaver, L., Marsh, D., Gris, D., Meakin, S. & Dekaban, G. (2002) Central mechanisms for autonomic dysreflexia after spinal cord injury. *Progress in brain research*, **137**, 83-95
- Wehrwein, E.A., Orer, H.S. & Barman, S.M. (2016) Overview of the Anatomy, Physiology, and Pharmacology of the Autonomic Nervous System. Compr Physiol, **6**, 1239-1278.
- Widmaier, E.P., Raff, H., Strang, K.T. (2014) Vander's Human Physiology: The Mechanisms of Body Function, 13th ed. New York: McGraw-Hill.
- Witzemann, V. (2007) Choline Acetyltransferase. In Enna, S.J., Bylund, D.B. (eds) *xPharm: The Comprehensive Pharmacology Reference*. Elsevier, New York, pp. 1-5.
- Yip, Y.P., Mehta, N., Magdaleno, S., Curran, T., & Yip, J.W. (2009) Ectopic expression of reelin alters migration of sympathetic preganglionic neurons in the spinal cord. *Journal of Comparative Neurology*, **515**, 260–268.
- Yip, Y.P., Zhou, G., Capriotti, C., & Yip, J.W. (2004) Location of preganglionic neurons is independent of birthdate but is correlated to reelin-producing cells in the spinal cord. *Journal of Comparative Neurology*, **475**, 564–574.
- Yogev-Seligmann, G., Hausdorff, J.M. & Giladi, N. (2008) The role of executive function and attention in gait. *Mov Disord*, **23**, 329-342; quiz 472.
- Zavvarian, M.-M., Hong, J. & Fehlings, M.G. (2020) The Functional Role of Spinal Interneurons Following Traumatic Spinal Cord Injury. *Frontiers in Cellular Neuroscience*, **14**.
- Zhang, F.-X., Ge, S.-N., Dong, Y.-L., Shi, J., Feng, Y.-P., Li, Y., Li, Y.-Q. & Li, J.-L. (2018) Vesicular glutamate transporter isoforms: The essential players in the somatosensory systems. *Progress in Neurobiology*, **171**, 72-89.
- Zhang, H., Shevtsova, N.A., Deska-Gauthier, D., Mackay, C., Dougherty, K.J., Danner, S.M., Zhang, Y. & Rybak, I.A. (2022) The role of V3 neurons in speed-dependent interlimb coordination during locomotion in mice. *eLife*, **11**, e73424.
- Zhang, Y., Narayan, S., Geiman, E., Lanuza, G.M., Velasquez, T., Shanks, B., Akay, T., Dyck, J., Pearson, K., Gosgnach, S., Fan, C.M. & Goulding, M. (2008) V3 spinal neurons establish a robust and balanced locomotor rhythm during walking. Neuron, **60**, 84-96.
- Zholudeva, L.V., Abraira, V.E., Satkunendrarajah, K., McDevitt, T.C., Goulding, M.D., Magnuson, D.S.K. & Lane, M.A. (2021) Spinal Interneurons as Gatekeepers to Neuroplasticity after Injury or Disease. J Neurosci, **41**, 845-854.
- Ziskind-Conhaim, L. & Hochman, S. (2017) Diversity of molecularly defined spinal interneurons engaged in mammalian locomotor pattern generation. J Neurophysiol, **118**, 2956-2974.

# Appendix

**Tris-EDTA buffer recipe for antigen retrieval:**

- Trizma base 1.21 g (10mM)
- EDTA 0.37 g (1mM)
- Distilled $H_2O$ up to 1 L
- Warm solution and mix until dissolved
- Adjust pH to 9.0
- Add 500 μL of Tween 20 and mix
- Store in fridge for up to 6 months

**Table 1: List of items and reagents**

| ITEM | Company | Cat # |
|---|---|---|
| ChAT anti gt | Millipore | AB114P |
| Living Colors DsRed Polyclonal Antibody | TaKaRa | 632496 |
| Alexa Fluor 488 anti gt | Invitrogen | A-11055 |
| VGlut2 anti gp | Millipore | AB2251-I |
| Alexa Fluor 647 anti gp | Jackson ImmunoResearch | 706-605-148 |
| Streptavidin Alexa Fluor 488 Conjugate | ThermoFisher | S-11223 |
| Streptavidin Alexa Fluor 647 Conjugate | ThermoFisher | S-21374 |
| Cy3 anti rb | Jackson ImmunoResearch | 711-165-152 |
| Dextran, Biotin, 10,000 MW, Lysine Fixable (BDA-10,000) | Invitrogen | D1956 |
| Normal donkey serum | Jackson ImmunoResearch | 017-000-121 |
| Cholera Toxin Subunit B (Recombinant), Alexa Fluor™ 488 Conjugate | Molecular Probes | C34775 |
| Tissue Tek OCT | Sakura | 4583 |
| Superfrost Plus Microscope Slides | Fisher Scientific | 12-550-15 |
| MX35 Premier+ Microtome Blades | ThermoScientific | 3052835 |
| ImmEdge Pen | Vector Laboratories | H-4000 |
| Microscope Glass Covers | Fisher Scientific | 12-545F |
| VECTASHIELD HardSet Antifade Mounting Medium | Vector Laboratories | H-1400 |
| PBS Tablets, Phosphate Buffered Saline | Fisher BioReagents | BP2944100 |
| Triton X-100 | Sigma-Aldrich | T9284-500ML |
| Trizma Base | Sigma-Aldrich | T1503-1KG |
| Ethylenediaminetetraacetic Acid, Di Na Salt Dihydr. (EDTA) | Fisher BioReagents | BP120500 |
| Tween 20 | Fisher BioReagents | BP337500 |
| Paraformaldehyde 16% w/v aq. soln methanol free | Alfa Aesar | 43368-9M |
| Isoflurane USP | Fresnius Kabi | CP0406V2 |
| IMARIS | Bitplane Software | |

| | | |
|---|---|---|
| Accumet Basic AB15 pH Meter | Fisher Scientific | 13-636-AB15 |
| Sucrose | Fisher Scientific | S5-3 |
| Glycerol | Sigma-Aldrich | G62779-1L |
| 75 RN SYR 5 uL Hamilton Syringe | Hamilton | 7634-01 |
| Single-Barrel Borosilicate Capillary Glass With Microfilament | A-M Systems Inc. | 601000 |
| Taper Point Vicryl + Antibacterial Suture | Ethicon | ETHVCP303H |
| Hydrochloric Acid 1.00 Normal | Fisher Scientific | 3700-1 |

**Table 2: List of Antibodies and RRIDs**

| Antibody | Company | RRID |
|---|---|---|
| ChAT anti gt | Millipore | (Millipore Cat# AB114P, RRID:AB_2313845) |
| Living Colors DsRed Polyclonal Antibody | TaKaRa | (Takara Bio Cat# 632496, RRID:AB_10013483) |
| Alexa Fluor 488 anti gt | Invitrogen by ThermoFisher | (Molecular Probes Cat# A-11055, RRID:AB_2534102) |
| VGlut2 anti gp | Millipore | (Millipore Cat# AB2251-I, RRID:AB_2665454) |
| Alexa Fluor 647 anti gp | Jackson ImmunoResearch | (Jackson ImmunoResearch Labs Cat# 706-605-148, RRID:AB_2340476) |
| Streptavidin Alexa Fluor 488 Conjugate | ThermoFisher | (Thermo Fisher Scientific Cat# S-11223) |
| Streptavidin Alexa Fluor 647 Conjugate | ThermoFisher | (Thermo Fisher Scientific Cat# S-21374, RRID:AB_2336066) |
| Cy3 anti rb | Jackson ImmunoResearch | (Jackson ImmunoResearch Labs Cat# 711-165-152, RRID:AB_2307443) |
| Dextran, Biotin, 10,000 MW, Lysine Fixable (BDA-10,000) | Invitrogen by ThermoFisher | (Thermo Fisher Scientific Cat# D1956, RRID:AB_2307337) * not an antibody |
| Normal donkey serum | Jackson ImmunoResearch | (Jackson ImmunoResearch Labs Cat# 017-000-121, RRID:AB_2337258) |
| Cholera Toxin Subunit B (Recombinant), Alexa Fluor™ 488 Conjugate | Molecular Probes | *not an antibody |

## Post-Surgery Score Sheet Parameters

**A**: Weight: Current weight

**B**: Weight change: (compared to the weight before surgery)
score: 0 ← 0-3 % weight decrease
1 ← 3 ≤ 10 %
2 ← 10 -15 %
3 ← >15 %

**C**: Appearance (fur, eyes…)
score: 0 ← shiny coat, clear eyes
1 ← fur a bit scruffy; eyes not clean (yellow mucus)
2 ← light piloerection, dehydration (skin tent present)
3 ← strong piloerection

**D**: Behavior
score: 0 ← normal (bright, alert, responsive)
1 ← tense and nervous at handling
2 ← no personal hygiene, apathetic
3 ← clearly stressed at handling: shivering, audible sounds ("painful squeaking"), aggressive behavior
AA ← automutilation (e.g. gnawing toes)

**E:** Motor activity
score: 0 ← normal
1 ← reduced activity, but no motor alterations
2 ← uncertain gait, problems with coordination
AA ← persistent immobility, not moving > 1 hr

**F**: Respiration
score: 0 ← normal respiration pattern, 100-200 /min
1 ← increased frequency
2 ← intense breathing, reinforced thoracal/ abdominal respiration*****

**G:** Application-related symptoms
score: 0 ← no
1 ← swelling in the head and neck region
AA ← paralysis
AA ← breaking off of the implant

**(AA = absolute abort criterion, the animal will be immediately euthanized with isofluorane overdose, followed by cervical dislocation)**

* Animal will be monitored every 15 min and given supportive measures (buprenorphine/meloxicam, additional fluids s.c., placed on a heating blanket, etc.). If no improvement within 2 hours, the animal will be immediately euthanized. Contact a veterinarian for further support.

**Table 3**: Post-surgical monitoring schedule based on scores.

| Score | Time interval of monitoring | Assessment | Measures |
|---|---|---|---|
| 0 | 3x/week | no constraint | None |
| < 5; no single value > 1 | every 24 hr | low constraint | careful observation, supportive measures (e.g. local antibiotic treatment, saline or 5% glucose injections) |
| > 5 or single value > 1 | 2x/day | medium constraint | analgesia (buprenorphine (morning and evening) + meloxicam (evening)), supportive measures (see above). Contact animal care staff and vet services of the helath status. If score does not improve within 48 hr, the animal is euthanized. |
| Single value > 2 | 3x/day | high constraint | If score does not improve within 24 hr, the animal is euthanized. |
| AA | NA | NA | Immediate euthanasia |